Linköping University | Department of Physics, Chemistry and Biology
Master's thesis, 30 hp | Chemical Biology, M Sc in Engineering
Spring 2020 | LITH-IFM-x-EX—20/3779--SE

GIANT UNILAMELLAR VESICLES FOR PEPTIDE-MEMBRANE INTERACTION STUDIES USING FLUORESCENCE MICROSCOPY

Martin Nilsson

Examinator, Daniel Aili
Tutor, Johanna Utterström
Tutor, Robert Selegård

LINKÖPINGS UNIVERSITET

Avdelning, institution
Division, Department

Department of Physics, Chemistry and Biology
Linköping University

Datum

Date

2020-07-07

Språk
Language

☐ Svenska/Swedish
☒ Engelska/English
☐ _____

Rapporttyp
Report category

☐ Licentiatavhandling
☒ Examensarbete
☐ C-uppsats
☐ D-uppsats
☐ Övrig rapport

☐ _____

ISBN

ISRN: LITH-IFM-x-EX—20/3779--SE

_____

Serietitel och serienummer **ISSN**

Title of series, numbering _____

URL för elektronisk version

Titel
Title

GIANT UNILAMELLAR VESICLES FOR PEPTIDE-MEMBRANE INTERACTION STUDIES USING FLUORESCENCE MICROSCOPY

Författare
Author

Martin Nilsson

Sammanfattning

Abstract

Vesicles are a type of biological or biomimetic particle consisting of one or more often spherical bilayers made up of amphipathic molecules, creating a closed system. They can function as an encapsulating device, holding hydrophilic molecules on the inside of the bilayer membrane(s) or hydrophobic molecules in the non-polar interstitial space in the middle of the bilayers. Because of this capacity to carry molecules, vesicles are a premier system for drug delivery and even theranostics in vivo. A peptide-based approach to release of encapsulated molecules has previously been developed but since drug delivery vesicles are in the size range of nanometers, the mechanisms have not been visualized. This project aims to produce giant unilamellar vesicles as a model system used to visualize membrane interactions vital to the understanding and further development of smaller vesicle-based systems for drug delivery. Giant unilamellar vesicles were produced successfully and a preparation protocol was established. Additionally, some membrane interactions were investigated using fluorescence microscopy.

Nyckelord
Keyword

Giant unilamellar vesicles, lipid rafts, fluorescence microscopy, drug delivery.

Abstract

Vesicles are a type of biological or biomimetic particle consisting of one or more often spherical bilayers made up of amphipathic molecules, creating a closed system. They can function as an encapsulating device, holding hydrophilic molecules on the inside of the bilayer membrane(s) or hydrophobic molecules in the non-polar interstitial space in the middle of the bilayers. Because of this capacity to carry molecules, vesicles are a premier system for drug delivery and even theranostics in vivo. A peptide-based approach to release of encapsulated molecules has previously been developed but since drug delivery vesicles are in the size range of nanometers, the mechanisms have not been visualized. This project aims to produce giant unilamellar vesicles as a model system used to visualize membrane interactions vital to the understanding and further development of smaller vesicle-based systems for drug delivery. Giant unilamellar vesicles were produced successfully and a preparation protocol was established. Additionally, some membrane interactions were investigated using fluorescence microscopy.

Abbreviations

MPB-PE – 1,2-dioleoyl-sn-glycero-3-phosphoethanolamine-N-[4-(p-maleimidophenyl)butyramide]

Liss-Rhod-PE – 1,2-dioleoyl-sn-glycero-3-phosphoethanolamine-N-(lissamine rhodamine B sulfonyl)

POPC – 1-palmitoyl-2-oleoyl-glycero-3-phosphocholine

CF – Carboxyfluorescein

Chol – Cholesterol

Cy5 – Cyanine 5

GUV – Giant unilamellar vesicle

ITO – Indium tin oxide

MMP-7 – Matrix metalloproteinase-7

mol% – Mole percent

LCO – Luminescent-conjugated oligothiophene

LUV – Large unilamellar vesicle

pFTAA – Penta-formylthiophene acetic acid

PBS – Phosphate buffered saline

PEG – Polyethylene glycol

PTFE – Polytetrafluoroethylene

Contents

1. Introduction

Liposomes, or vesicles, are (usually) nanoscale particles made up of lipid bilayer membranes. These membranes are made up of the same kinds of amphipathic lipid molecules as cells, and other materials, molecules and liquids can be stored within the space encapsulated by the membranes. Formation of vesicles occurs naturally in cells where they facilitate transport by liposome encapsulation. Vesicle mediated transport occurs both within single cells and between cells in multicellular organisms (De Jong *et al.*, 2019). Not only cells can produce vesicles, but they can be synthesized as well. Vesicles are supramolecular structures formed by hydrophobic interactions between amphipathic lipids and the surrounding polar solution (typically water), creating a system where some of the solvent is encapsulated on the inside of the vesicle, with polar lipid headgroups interacting both with the outside and the inside solvent molecules. The non-polar fatty acids in both lamella are facing each other and once formed are vesicles are stabilized by Van der Waals interactions between non-polar moieties as well as electrostatic interactions between polar moieties and solution. Not only can vesicles be synthesized with natural components, but synthetic amphipathic molecules can be incorporated as well (Dimova and Marques, 2019). Several methods of vesicle formation will be described further in this report.

Naturally the capacity of liposomes to facilitate molecular transport in living organisms is of great interest for medical purposes, particularly in the field of drug delivery. Drug delivery refers to various systems for introducing therapeutic agents into a patient, and then regulating transport and release of the agent. “Drug delivery system is an interface between the patient and the drug.” (Jain, 2020). Drug delivery systems can for example facilitate localization to specific tissues via ‘drug delivery vehicles’. Vesicles are a common option for drug delivery with two major advantages: biocompatibility due to similarity with cellular membranes, and capacity to tune drug release over time to fit therapeutic range (Bozzuto and Molinari, 2015). The release may be due to biodegradation, but a release mechanism triggered by specific circumstances may be of great use for drug delivery.

The peptides JR2K and JR2E are helix-loop-helix peptides forming a four-helix bundle when heterodimerized with each other (Rydberg, Baltzer and Sarojini, 2013). Originally developed by Rydberg, Balzer and Sarojini (2013), JR2K has been modified by the laboratory of molecular materials at Linköping university to contain a cysteine residue in the loop region (Lim *et al.*, 2016) and is one of many peptides developed and modified by this group (Skyttner *et al.*, 2018,

2019). The cysteine containing version of JR2K is known as JR2KC, and similarly to naturally occurring antimicrobial peptides, JR2KC has been found to release membrane encapsulated molecules when bound to a membrane (Lim *et al.*, 2016). JR2KC was bound to the membrane by the cysteine residue present in the JR2KC peptide covalently binding to maleimide moieties in 1,2-dioleoyl-sn-glycero-3-phosphoethanolamine-N-[4-(p-maleimidophenyl)butyramide] (MPB-PE) lipid molecules constituting part of the synthetic membrane. The complementary peptide JR2E, was investigated as an inhibitor for JR2KC mediated membrane release (Lim *et al.*, 2016). When in this heterodimer form the JR2KC peptide could not release carboxyfluorescein (CF) encapsulated in liposomes. JR2E was also designed with two target motifs for the proteolytic enzyme matrix metalloproteinase-7 (MMP-7), which was used as the triggering factor to activate JR2KC: MMP-7 introduces breaks into the primary sequence of JR2E which then is unable to bind JR2KC, and in turn JR2KC binds to membrane and releases the molecules contained within (Lim *et al.*, 2016). Since MMP-7 is upregulated and excreted by many cancer cell types (Szarvas *et al.*, 2010), this system could be used to transport anticancer drugs to cancer tissues by liposome, and have local drug release (Lim *et al.*, 2016). This system could potentially be developed into a theranostics system (combined diagnosis and therapy in a single system) (Bozzuto and Molinari, 2015), where an anti-cancer is released along with a traceable indicator, which can be detected to diagnose and monitor the cancer while treating it at the same time.

This system has been thoroughly quantified: Release efficiency by JR2KC, along with JR2E inhibition and MMP-7 activation has been studied by tracking (CF) fluorescence when released from the liposomes (loaded at quenching concentrations). JR2KC secondary structure change in pore formation has been investigated by circular dichroism spectroscopy, and JR2KC interactions with the lipid membrane have been studied by quartz crystal microbalance (Lim *et al.*, 2016). New and yet unpublished studies of the system by the laboratory of molecular materials have been made, and some of the results have prompted the undertaking of this study.

First it has been discovered that inclusion of cholesterol (Chol) in the liposomes induces a more effective release. Normally the liposomes studied consist of 95 mole-percent (mol%) 1-palmitoyl-2-oleoyl-glycero-3-phosphocholine (POPC) and 5 mol% MPB-PE. However with 30 mol% cholesterol (Chol), 65 mol% POPC and 5 mol% MPB-PE the rate of (CF) release from the liposomes is increased. It is hypothesized that this is due to formation of lipid rafts in the liposome membrane. Lipid rafts are a concept first proposed by Simons and Ikonen (1997) and has to do with the interactions of membrane phospholipids, cholesterol, and peptides or

proteins. Lipid membranes can consist of several phases such as liquid-ordered, liquid-disordered, and solid, and these phases can exist simultaneously in separate phases of the same membrane. As membranes are essentially a two-dimensional environment with respect to their constituent molecules, this phenomenon is called lateral phase separation (Wheeler and Tyler, 2011). Lipid rafts are one type of phase separation where membrane interacting proteins or peptides form domains in the membrane along with specific ordering of membrane lipids, often with multiple proteins of the same or different types in the same rafts (Simons and Ikonen, 1997). Organization of lipid rafts may be dependent on the ability of cholesterol to condense lipids in the membrane (Veatch and Keller, 2002), and interactions between cholesterol and at leas two phospholipids have shown to generate multiple different phase separations (Veatch and Keller, 2003). It is however still unclear in which order rafts form – do they form around proteins/peptides interacting with the membrane, or are proteins/peptides specifically recruited to pre-formed domains, or something in between (Levental and Veatch, 2016)?

The laboratory of molecular materials have also found that luminescent-conjugated oligothiophenes (LCOs) are able to inhibit membrane permeabilization by JR2KC. Specifically the LCO penta-formylthiophene acetic acid (pFTAA) has been observed to inhibit at a concentration of 20:1 [pFTAA:JR2KC]. LCOs are fluorescent molecules which have been shown to bind amyloid Aβ plaques, a toxic peptide and biomarker for Alzheimer's disease. The LCOs can reduce toxicity by inducing a conformation change to Aβ fibrils (Civitelli *et al.*, 2016). This could be developed with the JR2KC-liposome drug delivery vehicle to a drug delivery system for Alzheimer's disease.

The purpose of this project was to study the findings in the previous two paragraphs visually using fluorescence microscopy: To gather footage supporting or disproving lipid raft formation in cholesterol containing liposomes and though this study was not performed to study the causes of raft formation it may provide interesting insight. The other purpose was to visualize pFTAA inhibition of JR2KC in conjunction with liposomes. However, the liposomes used in previous studies have been in the nm scale; such liposomes are considered large unilamellar vesicles (LUVs) and are far too small to visualize in any optic microscope. In order to study them visually giant unilamellar vesicles (GUVs) of the same composition needed to be produced. Giant unilamellar vesicles have a diameter in the µm size range, usually 1-50 µM but even larger can be formed (Dimova and Marques, 2019). Other than size there are no fundamental differences between LUV and GUVs in terms of the supramolecular forces holding them together or molecular compositions, but the preparation methods for GUVs are different from

those for LUV, which is further discussed in the methods section. This led to the need to establish a protocol for GUV formation usable with the same lipids and solution conditions as with the previously studied liposomes, to enable fluorescence microscopy in this project and further investigations for the drug-delivery system. A fluorophore also needed to be incorporated to visualize the GUVs in fluorescence microscopy; the fluorescently labeled phospholipid 1,2-dioleoyl-sn-glycero-3-phosphoethanolamine-N-(lissamine rhodamine B sulfonyl) (Liss-Rhod-PE) was used, and is further explained in the materials section.

1.1 Aim

The objectives of this project were: **(1)** To establish a protocol for formations of GUVs with the compositions 65:5.30 [POPC:MPB-PE:Chol] and 95:5 [POPC:MPB-PE], along with a small mol% Liss-Rhod-PE. **(2)** To study formation of lipid rafts and JR2KC binding using fluorescence microscopy. **(3)** To examine inhibition and binding by LCOs to JR2KC using GUVs and fluorescence microscopy.

1.2 Purpose

The reason for this project's commission was to create supporting data and procedures in order to facilitate further development of a vesicle-JR2KC interaction-based drug delivery system.

2. Materials and Methods

This section of the report describes the theoretical background of methods used in the project and details the use of these methods in the thesis project. The methods described here are the final versions employed to yield the results in section 3 and were refined to this point during the course of the project.

2.1 Theory

In this section theoretical basis of the methods employed during the work is described.

2.1.1 Gentle hydration

The method of GUV preparation known as gentle hydration, or spontaneous swelling is the oldest method for GUV preparation (Dimova and Marques, 2019). It was created by Reeves and Dowben in 1969 (Reeves and Dowben, 1969), but currently a method called electroformation is by far the most common to generate GUVs, although gentle hydration is still useful in the right circumstances. Gentle hydration is a method based on swelling from lipid films into large liposomes and has essentially three steps, illustrated in figure 1: A) Lipids

are spread on a surface and dried to form a lipid film. B) The lipid film is slightly rehydrated but stays in place and acts as a thin film on a surface still. C) The film is submerged in a solution, and over time buds out and forms GUVs. Lipid films are often dried ether directly on the glass of a beaker (Reeves and Dowben, 1969; Akashi *et al.*, 1996, 1998; Shimokawa *et al.*, 2010) or on polytetrafluoroethylene (PTFE) sheets (Manley and Gordon, 2008; Kubsch *et al.*, 2017). The rehydration step is generally either performed by exposing the dried lipid films to steam (Kubsch *et al.*, 2017) or to water saturated nitrogen gas (Reeves and Dowben, 1969; Akashi *et al.*, 1996, 1998; Manley and Gordon, 2008). In the end water saturated nitrogen was used for this project, but a steam setup was initially tried, described in appendix A and illustrated in figure A1. The swelling solution is usually an aqueous solution that is not too biologically harmful, frequently sugar based solutions are commonly used and considered effective for gentle hydration (Tsumoto *et al.*, 2009).

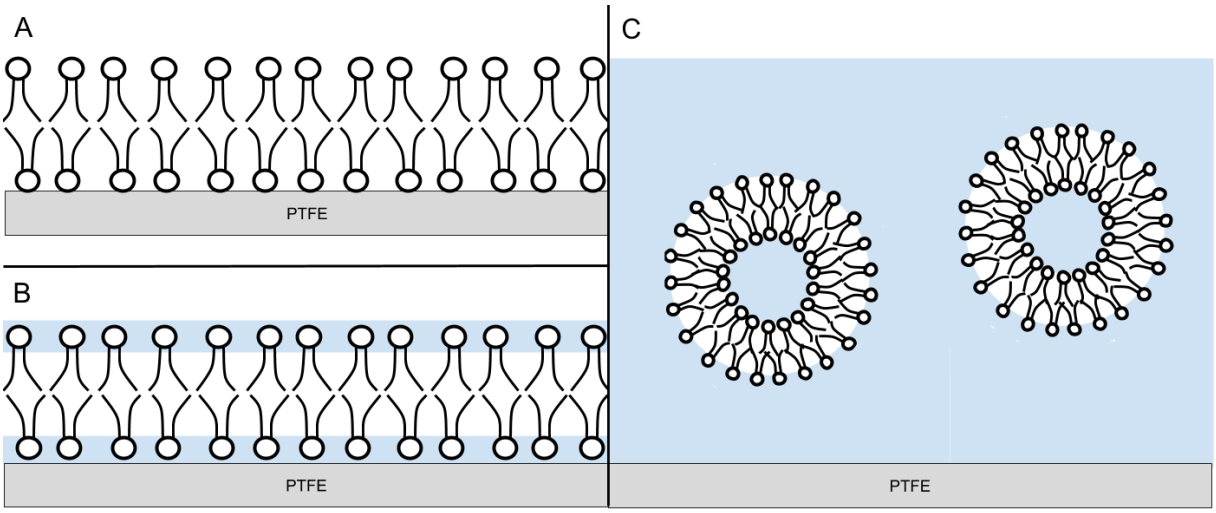

Figure 1. Graphical depiction of the key steps in gentle hydration. A: Dried lipid film on PTFE sheet. B: Slightly rehydrated lipid film, still on the sheet. C: GUVs have formed after the film has been submerged in aqueous solution.

Gentle hydration has two major drawbacks; it takes a long time, at least 24 hours, and will always produce non-GUV debris structures (Dimova and Marques, 2019). In contrast electroformation is rapid, taking only a few hours and has a good yield of GUVs (Méléard, Bagatolli and Pott, 2009). Electroformation is also based on dried lipid films, but the films are dried on an electrode in this case, no rehydration is required, and the swelling occurs due to a voltage being run through swelling media in contact with the electrodes. The electrodes are most often indium tin oxide (ITO) coated glass slides, which are convenient for microscopy (Méléard *et al.*, 1997). However there are two weaknesses with electroformation which made

it problematic for the purposes of this work; it does not handle either strong saline solutions well (Méléard, Bagatolli and Pott, 2009), nor does it work well with charged lipids (Steinkühler *et al.*, 2018). Gentle hydration is also not amenable to high ion strength solutions, but GUVs can reliably be prepared in such conditions using gentle hydration (Akashi *et al.*, 1996; Stein *et al.*, 2017). There are ways of making electroformation work with high saline concentrations, but they usually require expensive platinum wire electrodes to be used (Pott and Philippe, 2008). Some proprietary methods use cheaper materials as electrodes, but require elaborate and hard to construct formation chambers either way (Pereno *et al.*, 2017). Inability to perform in high saline conditions was a problem for the purposes of this work; since the liposome-JR2KC system is made to eventually be utilized in vivo all previous studies have been performed in physiologically relevant conditions with phosphate buffered saline as the working solution in which liposomes are dispersed (Lim *et al.*, 2016). Therefore, being able to use PBS as the swelling solution for GUVs was a priority in this project.

Formation of intracellular structures and membrane composition asymmetries during electroformation of GUVs containing charged lipids (Steinkühler *et al.*, 2018) would be detrimental to the project, as all GUV compositions this project aimed to produce contained 5 mol% MPB-PE, a negatively charged lipid. In the case of gentle hydration however, inclusion of charges in the lipid film is actually a requirement for the method to work (Reeves and Dowben, 1969; Akashi *et al.*, 1998). Budding of GUVs in the is caused by the swelling solution. Budding occurs because of the swelling solution flowing between the lipid lamellae due to osmotic pressure, enhanced by the rehydration step (figure 1) (Tsumoto *et al.*, 2009), and because of electrostatic repulsion between charged species in the lipid bilayer helping the lamellae to separate and take shape as GUVs (Akashi *et al.*, 1998).

2.1.2 Fluorescence microscopy

In fluorescence microscopy fluorescent markers are employed to visualize structures and interactions during microscopy (Bagatolli, 2006; Wheeler and Tyler, 2011; Dimova and Marques, 2019). The main label for GUVs was Liss-Rhod-PE, containing a fluorescent rhodamine moiety, and with the same fatty acid moieties as the JR2KC binding MPB-PE. In some instances, pFTAA bound to cholesterol via a polyethyleneglycol (PEG) linker was incorporated into GUV lipid composition and used as a fluorescent marker for GUVs. Being able to observe JR2KC at GUV membranes would be useful in correlating phase separation and lipid binding. To this end JR2KC was labeled with Cyanine 5 (Cy5) using NHS chemistry, binding Cy5 to amine groups on JR2KC. Since JR2KC contains 12 lysine (K) residues and an

N terminal, Cy5 has many possible binding spots. As described in section 2.2.3 a 1:1 ratio of JR2KC to Cy5 was used during labelling, which could mean that individual JR2KC molecules could have a varying number of Cy5 bound to them. Theoretically this could range from some JR2KC molecules binding no Cy5 moieties to complete saturation of amine groups by Cy5 on other JR2KC molecules.

In order to observe GUVs in microscopy during longer periods, and especially if one wishes to introduce substances and observe changes in one GUV due to interaction, the GUVs need to be immobilized. For this work the a method using agarose with low gelling temperature has been employed (Lira *et al.*, 2016). According to Lira et al. (2016) GUVs dispersed in 0.5% w/v agarose gel are completely immobilized and remain so even after addition of new solution volume onto the gel. This could be utilized to record changes in the same GUV before, during, and after JR2KC is introduced to it. There are other methods for GUV immobilization, such as binding the vesicles to a bottom covered in avidin via biotinylated lipids in the GUV (Dimova and Marques, 2019), however such immobilization would be disruptive to the internal organization of membrane lipids (Sarmento, Prieto and Fernandes, 2012).

2.2 Experimental section

In this section the experimental details leading to the results presented in section 3 are presented, starting with a recounting of materials and equipment.

JR2KC peptide (sequence: NAADLKKAIKALKKHLKAKGPCDAAQLKKQLKQAFKAFK RAG) and JR2K peptide (sequence: NAADLKKAIKALKKHLKAKGPVDAAQLKKQLKQ AFKAFKRAG) were synthesized at the laboratory of molecular materials, Division of Physics, Dept. of Physics, Chemistry and Biology, Linköping University, using SPPS chemistry. Sulfo-Cyanine5 (Cy5) NHS ester was purchased from Lumiprobe. The lipids 1-palmitoyl-2-oleoyl-glycero-3-phosphocholine (16:0-18:1 PC | POPC), 1,2-dioleoyl-sn-glycero-3-phosphoethanolamine-N-[4-(p-maleimidophenyl)butyramide] (sodium salt) (18:1 MPB PE), 1,2-dioleoyl-sn-glycero-3-phosphoethanolamine-N-(lissamine rhodamine B sulfonyl) (ammonium salt) (18:1 Liss Rhod PE) and cholesterol (plant derived) were purchased from Avanti Polar Lipids, Inc. and dissolved in chloroform. The LCO pentameric formyl thiophene acetic acid (pFTAA) and PEG linked pFTAA-Chol as kindly provided by the group of Prof. Peter Nilsson, Division of Chemistry, Dept. of Physics, Chemistry and Biology, Linköping University. Agarose, low gelling temperature (2-Hydroxyethyl agarose) was purchased from Sigma-Aldrich. PBS was made from PBS tablets dissolved in MilliQ water; pH adjusted with

HCl. For lipid in chloroform solutions 50 µl and 10 µl Hamilton syringes were used. MILLEX GV 0.22 µM filter units for plastic syringes were employed. Polytetrafluoroethylene (PTFE, commonly known as Teflon) sheet of 1.5 mm thickness, white, was purchased from VWR. 96 well cell culture microplate, black, flat bottom µClear, sterile was purchased from Greiner Bio-One. Single use size exclusion column, GE healthcare PD MiniTrap G-10 column was purchased from Sigma-Aldrich.

For fluorescence microscopy a modular widefield fluorescence microscope outfitted for TIRF was used. The microscope base mount was a Nikon Eclipse Ti inverted microscope, running NIS Elements AR software. Fluorescence excitation from a mercury EPI-Fl illuminator: Nikon intensilight C-HGFIE, equipped with neutral density (ND) shutter. The objective used for imaging was a Nikon S Plan Fluor ELWD 60x DIC N1. A Nikon DS-Fi2 camera was used to record images and time-lapses. Three filter cubes were used for fluorescence microscopy: TIRTC filter cube with a 556-∞ nm wavelength dichroic mirror, an excitation filter for 528-553 nm and an emission filter for 590-650 nm. Cy5 filter cube with a 625-∞ nm wavelength dichroic mirror, an excitation filter for 625-650 nm and an emission filter for 672-716 nm. Aqua Longpass filter cube with a 455-∞ nm wavelength dichroic mirror, an excitation filter for 400-440 nm and an emission filter for 465-∞ nm.

2.2.1 GUV preparation

Since one of the aims of this work was to create a protocol for GUV preparation, the protocol is considered a result for the purposes of this report. Specific experimental details are provided in this section but will refer to Protocol 1 in section 3.1.

Lipid stock solutions were previously prepared in chloroform, and from these stock solutions three lipid mixtures for GUVs were prepared (step 1 of protocol 1). For GUV of composition 64.5:5:0.5:30 [POPC:MPB-PE:Liss-Rhod-PE:Chol] 136.9 µl chloroform, 42.9 µl of 10 mg/ml POPC stock, 4.4 µl of 10 mg/ml MPB-PE stock, 5.7 µl of 1 mg/ml Liss-Rhod-PE stock, and 10.2 µl of 10 mg/ml Chol stock were mixed for a total lipid concentration of 4mM. For GUV of composition 94.5:5:0.5 [POPC:MPB-PE:Liss-Rhod-PE] 133.5 µl chloroform, 57.5 µl of 10 mg/ml POPC stock, 4.0 µl of 10 mg/ml MPB-PE stock, and 5.2 µl of 1 mg/ml Liss-Rhod-PE stock were mixed for a total lipid concentration of 4mM. For GUV of composition 65:5:29.5:0.5 [POPC:MPB-PE:Chol:pFTAA-Chol] 262.7 µl chloroform, 79.7 µl of 10 mg/ml POPC stock,

8.1 µl of 10 mg/ml MPB-PE stock, 18.4 µl of 10 mg/ml Chol stock, and 1 µl of 10 mg/ml pFTAA-Chol stock were mixed for a total lipid concentration of 4mM.

2x2 cm^2 PTFE sample pads were prepared with P220 grit sandpaper as described in protocol 1 step 2 and were washed as specified in step 3. 15 µl of each GUV lipid mixture were spread on separate PTFE pads using Hamilton syringes and placed inside small glass beakers, with a volume of about 30 mL (figure B1 in Appendix B). These were covered by aluminum foil, which was pierced to give air holes, and then placed under vacuum in a desiccator for at least 4 hours to completely dry the lipid films (step 4 of protocol 1). During vacuum drying, the setup for generating water-saturated nitrogen was prepared, which is described in figures 2 and B2. After drying, the lipids were hydrated by water saturated nitrogen for 40 minutes in accordance with step 5 of protocol 1. After hydration 5 ml of PBS, pH 7.36 and preheated to 45 °C was deposited through a 22 µm syringe filter (to remove bacteria) into the beakers containing lipid films on PTFE pads, so that the lipid films were submerged. The beakers were covered by parafilm and placed in an oven at 45 °C overnight (step 6 of protocol 1). The next day GUVs were harvested into separate glass vials as described in step 7 of protocol 1, and were stored in a refrigerator at about 8 °C. 400 µl of each GUV solution was harvested, and assuming all lipid content was collected gives a concentration of:

$$\frac{Deposited\ lipid\ mix\ vol. * lipid\ mix\ conc.}{Collected\ GUV\ sample\ vol} \quad \frac{15\ \mu l * 4\ 000\ \mu M}{400\ \mu l} = 150\ \mu M\ GUV$$

2.2.2 GUV immobilization

As with the GUV formation protocol, studying membrane interactions of GUVs was an aim of this work. Since immobilization is required for such studies, protocol 2 was considered a result for the purposes of this report and can be found in section 3.2. Here the experimental details are presented. 20 ml PBS, pH 7.36 was heated to 80 °C and 207.9 mg 2-Hydroxyethyl agarose powder was dissolved by stirring, to a concentration of about 1% w/v. The dissolved gel was portioned into 500 µl aliquots in Eppendorf tubes and stored in a refrigerator at 8 °C.

To immobilize GUV samples in the wells of a 96 well plate, agarose needed to be liquid in order to mix with GUV samples. To this end agarose gel portions were heated to 75 °C in a water bath for 10 min, and then allowed to cool in a water bath of 40-45 °C. During this time 15 µl PBS, pH 7.36 was placed in each well, along with 10 µl of 150 µM GUV sample. Finally, 25 µl of 1% w/v agarose liquid from the water bath was mixed with the contents of each well by pipetting up and down a few times. The gel was then allowed to cool in a refrigerator for an hour. In total each well contained 50 µl of PBS, pH 7.36 based 0.5% w/v agarose gel with

GUVs dispersed in it, at a concentration of 30 µM. Two rows of the 96 well plate (12 wells in each row) were used for GUVs with the composition 64.5:5:0.5:30 [POPC:MPB-PE:Liss-Rhod-PE:Chol], and one row each were used for GUVs with the compositions 94.5:5:0.5 [POPC:MPB-PE:Liss-Rhod-PE] and 65:5:29.5:0.5 [POPC:MPB-PE:Chol:pFTAA-Chol].

2.2.3 Peptide labelling

In order to label JR2KC with Cy5, 200 µl of MilliQ water was mixed with 2.51 mg JR2KC (M = 5720 g/mol) and 0.37 mg Sulfo-Cyanine5 NHS ester (M = 777.95 g/mol) to an approximate 1:1 mixture in an Eppendorf tube. This sample was incubated at room temperature for 5 hours, covered in aluminum foil to block light. After this, the sample was filtered to remove Sulfo-Cyanine5 NHS ester which had not bound to JR2KC using a MiniTrap G-10 size exclusion chromatography column, collecting 500 µl sample.

The sample was calculated to have a concentration of 1 mM JR2KC-Cy5. The correct concentration was checked using Ellman's test. Ellman's test gives the concentration of free thiol groups in a solution, the effective concentration of JR2KC-Cy5 which can bind to MPB-PE in GUV membranes. Briefly, 840 µl MilliQ water, 50 µl of 2 mM DNTB, and 100 µl of 1 M, pH 8.0 Tris are mixed in a cuvette. Before sample is added, absorbance of the reagent mixture is measured in a UV spectrometer at 412 nm. 10 µl of the sample is added, mixed, and incubated for 5 min, and another absorbance measurement is made at the same wavelength. The concentration of unoxidized thiols is calculated as (assuming the cuvette is 1 cm wide): $[SH] = \frac{Sample\ abs. - Background\ abs.}{\varepsilon}$ where the extinction coefficient ε is 13 600 $M^{-1}cm^{-1}$.

After using the MiniTrap, the JR2KC-Cy5 (aq) stock solution was calculated to have the effective concentration 448.5 µM, and new tests were taken regularly between uses of the stock solution, which was stored in a freezer.

2.2.4 Widefield fluorescence microscopy

When recording immobilized GUVs through the camera an auto-exposure feature of NIS Elements AR software was used to give optimal images. Usually the exposure was set to 1 second, and analog gain to 4.0x, but would sometimes vary, which is presented in 3-23. The procedure for recording time lapses was to start a time lapse capture, wait for multiple images to be taken and then add peptides after usually 60 s. Generally, time-lapses consisted of images being captured automatically every 10 s for 5 min, although there were some exceptions. In each case, 5 µl of peptide solution would be carefully placed on top of the gel and allowed to seep into the gel. As mentioned in section 3.2 the GUVs could be slightly displaced by the

addition of solution to the gel, so the positioning and focus of the microscope needed to be adjusted during the capture.

For the results presented in figures 3-5, B3-7 and in text in section 3.2, the peptides JR2KC-Cy5 or JR2K were added from a 11 µM aqueous solution prepared from stock solutions of JR2KC-Cy5 (aq) made during this project, and previously prepared JR2K in MilliQ water solution. They were added to both 64.5:5:0.5:30 [POPC:MPB-PE:Liss-Rhod-PE:Chol] GUVs and 94.5:5:0.5 [POPC:MPB-PE:Liss-Rhod-PE] GUVs in wells. This means that each well, which contained 50 µl immobilized GUV suspension and 5 µl peptide after addition, had a concentration of 1 µM JR2KC-Cy5 or JR2K after addition. Mixtures of 11 µM JR2KC-Cy5 and 11 µM pFTAA (from stock solution in MilliQ) were added to both 64.5:5:0.5:30 [POPC:MPB-PE:Liss-Rhod-PE:Chol] GUVs and 94.5:5:0.5 [POPC:MPB-PE:Liss-Rhod-PE] GUVs in wells in order to yield 1 µM JR2KC-Cy5, 1 µM pFTAA in the presence of GUVs. The results are presented in figures 6, B8-B12 and text in section 3.2. Similarly, mixtures of 11 µM JR2KC-Cy5 and 220 µM pFTAA were also added to both 64.5:5:0.5:30 [POPC:MPB-PE:Liss-Rhod-PE:Chol] GUVs and 94.5:5:0.5 [POPC:MPB-PE:Liss-Rhod-PE] GUVs in order to yield 1 µM JR2KC-Cy5, 20 µM pFTAA in wells. These results are presented in figures B13-B16 and in text in section 3.2.

For the GUVs with composition 65:5:29.5:0.5 [POPC:MPB-PE:Chol:pFTAA-Chol] time-lapses were recorded during additions of 5 µl of 11 µM JR2KC. However, these were not presentable due to fast photobleaching of pFTAA. Time-lapses of the photobleaching were recorded and are presented in figures 7 and B21. Finally, a dilution series of JR2KC-Cy5 was examined. The peptide was diluted to be proportional to the amount of MPB-PE present in a well of the microplate. Using the same amount of 64.5:5:0.5:30 [POPC:MPB-PE:Liss-Rhod-PE:Chol] GUV sample as before, 10 µl of 150 µM GUVs diluted to 55 µl with 40 µl added PBS and 5 µl peptide sample would give a MPB-PE concentration of 1.5 µM, since MPB-PE constituted 5 mol%. Assuming that about half of the MPB-PE is turned to the inside of the GUVs, that means 0.75 µM MPB-PE available in the well. Peptide solutions were prepared to 8.2 µM, 1.64 µM, 0.82 µM, 0.55 µM and 0.41 µM; corresponding to 1:1, 1:5, 1:10, 1:15 and 1:20 [JR2KC-Cy5:Availiable MPB-PE] once 5 µl of one respective peptide solution was added to a well. In the case of this experiment a different batch of 64.5:5:0.5:30 [POPC:MPB-PE:Liss-Rhod-PE:Chol] GUVs were used. This batch had a lipid concentration of 120 µM, 10 µl of which was used in each well, and the volume of each well was filled out to 50 µl, giving a final GUV lipid concentration in the wells of 24 µM, and thus 0.6 µM available MPB-PE. Note that

this is the concentration of GUV lipids before any addition of JR2KC. This corresponded to 1:0.8, 1:4, 1:8, 1:12 and 1;16 [JR2KC-Cy5:Availiable MPB-PE] once 5 µl of one respective peptide solution was added to a well. The experiment procedure was as follows: 40 µl PBS, pH 7.36, and 10 µl of 64.5:5:0.5:30 [POPC:MPB-PE:Liss-Rhod-PE:Chol] was added to and mixed in 10 different wells on the 96 well microplate. Note that no immobilization was performed. 5 µl of ether 8.2 µM, 1.64 µM, 0.82 µM, 0.55 µM or 0.41 µM JR2KC-Cy5 (aq) were deposited separately in these wells and mixed, two wells for each peptide concentration. These were incubated for 20 min, and then investigated by fluorescence microscopy, the results of which are written at the end of section 3.2 and in figure 8.

3. Results

This section describes the primary results of this project pertaining to the main objectives described at the end of the introduction section of the report. Intermediary results during the project and process analysis are presented in appendix A.

3.1 GUV preparation

The primary objective of this project was to produce a reliable and reproducible method of producing GUVs for use in studying membrane interactions with fluorescence microscopy. Specifically, the lipid compositions of GUVs included 5 mol% of a negatively charged lipid (MPB-PE) in both cases, and 30% cholesterol in one composition, with the primary lipid being POPC (neutral charge). Additionally, a fluorescent probe (Liss-Rhod-PE) needed to be incorporated to facilitate fluorescence microscopy. Ideally, the GUVs were to be produced and suspended in PBS in order to be a realistic model for the smaller drug-delivery vesicles. This was successful on all counts, and resulting GUVs were used for fluorescence microscope imaging, presented in section 3.2.

The process of refining this method yielded a protocol for GUV preparation, Protocol 1, and a setup for hydrating lipid films with water-saturated nitrogen (figure 1) used in the same protocol. See appendix B for photographs of this setup. Utilizing water-saturated N_2 instead of water vapor to rehydrate dried lipid films before swelling to GUVs in PBS increased the overall yield of vesicles. It also enabled swelling with 5 mol% MPB-PE in PBS; before at least 10 mol% charged lipid was needed (Akashi *et al.*, 1996).

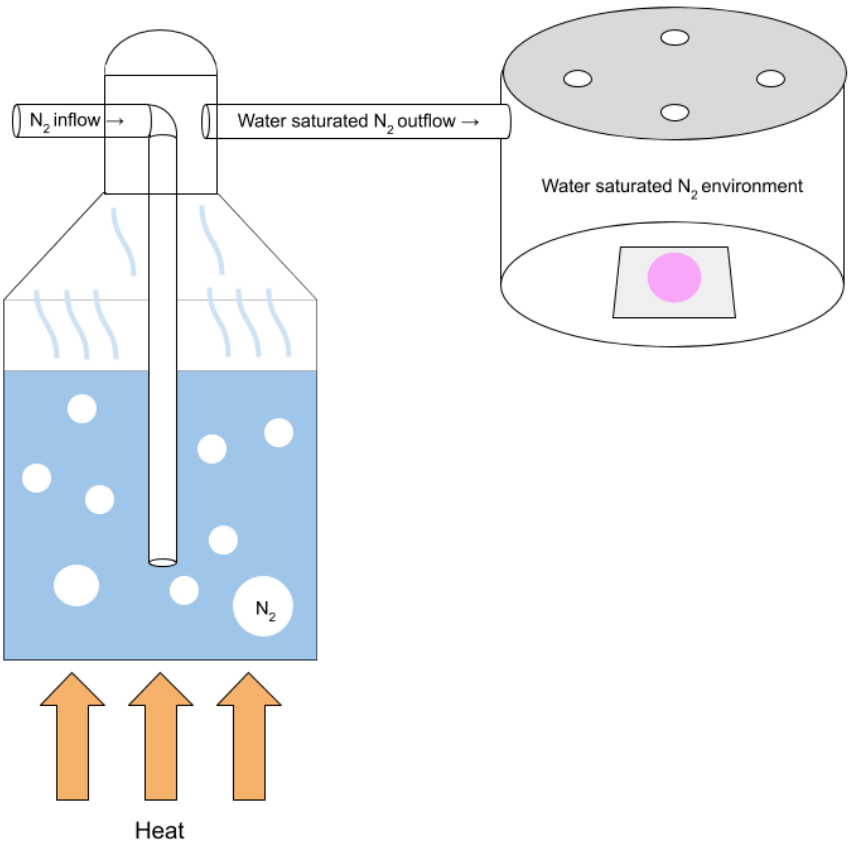

Figure 2. Schematic illustration of setup for dried lipid-layer rehydration by water-saturated N_2. N_2 is bubbled through Milli-Q water heated to near-boil point, generating water-saturated N_2 (left part of figure). Water-saturated N_2 is funneled into a chamber with hole vents in its lid, where dried lipid film can absorb water from the water-saturated N_2 environment.

Protocol 1 is the result of the first objective of this project and is intended to independently from this report describe the method developed to produce GUVs under the same or similar circumstances as used in this report. Because an objective of the project was to develop the protocol, it is presented in results, rather than in the methods section where a brief description is used instead.

Protocol 1: GUV preparation – gentle hydration method

The following protocol is variation of the gentle hydration method, also known as spontaneous swelling method of GUV formation. This variant of the method is specifically designed for two parameters; inclusion of charged lipids in the vesicle bilayer membrane, and preparation in PBS solution. For GUV preparation where those parameters are different this protocol may be of help but should be adapted to the specifics of such preparations.

1. Prepare lipid mixtures for the desired membrane composition in chloroform (or other suitable organic solvent) to a total lipid concentration of 4 mM. These mixtures need to contain a fraction of charged lipid, 5% (mol lipid) works but ideally 10% - 20% of the lipids should be charged. If several charged lipids are included, they should not have different charges since this method requires charge repulsion between lipids.
2. Prepare sample 'pads' for the lipid mixture. The pads can be cut out of a polytetrafluoroethylene (PTFE) sheet, to pieces about 2x2 cm^2 in area and thick enough to be rigid (≥1.5 mm). These pads should be rubbed with fine sandpaper (P220 and P320 grit both work) on one or both sides of the pad so that lipid samples don't slip off the pad. Small beakers in which sample pads can be placed and covered by 5 ml of fluid are necessary. If the pads don't fit, they can be made with a smaller area.
3. Wash sample pads and beakers with dishing soap and water, then rinse them in order with water, ethanol and finally chloroform.
4. Spread up to 15 µl lipid mixture on a sandpaper-treated side of a PTFE-pad, move the pad to a beaker using pincers and place it in a desiccator for at least two hours.
5. Rehydrate the lipid sample for at least half an hour with water saturated N_2 (A setup for this is described in figure 2). When the lipids are hydrated the lipid film should appear "glossy" in contrast to before the hydration. During this procedure, pre-heat the swelling solution (PBS) to the temperature for overnight swelling (see step 6).
6. Gently deposit 5 ml PBS (or other saline solution) into the beaker containing the PTFE-pad with hydrated lipids, using a syringe equipped with an 0.22 µm filter to remove any bacteria from the solution. Seal the beaker with parafilm, and place the beaker in an oven overnight at 45 °C.
7. The next day, let the solution cool to room temperature over 1 hour. When this is done, the GUV should be ready for harvest. This is usually indicated by small lumps floating in the solution. Use a pair of scissors to cut a pipette tip to get a hole large enough to harvest the lumps and use a piston pipette to transfer these to a suitable container. The gathered volume is up to the discretion of the protocol user. The GUV can be stored in a refrigerator for more than a week. Wash PTFE pads and beakers with acetone before reuse.

Troubleshooting: It is critical that GUV swelling in step 6 occurs at a temperature greater than the melting temperature of the lipids used. The recommended service temperature for parafilm is 50 °C or less, so at higher temperatures parafilm cannot be used to seal the beaker. It is important that the lipid solution is evenly spread when deposited on the PTFE-pad, if spin coating is available it is a good option. Try to limit lipid exposure to oxygen, since it may oxidize unsaturated lipids. Sometimes no lumps appear in step 7 even though the lipid film is visibly depleted, which can happen if the cooling goes on for too long. This means that vesicles have dissolved into the solution and can still be harvested from the solution. Cutting pipette tips may leave small contaminations in harvested GUV samples; wash them before harvesting by pipetting MilliQ water.

Comments: PTFE-pads may not be strictly necessary since lipids can be spread directly on glass, but sample handling is more convenient with pads. Including fluorescently labelled lipids (or other color-giving) molecules may aid visually in spreading on the PTFE-pads and when harvesting. This protocol will yield only a fraction of GUVs along with other lipid structures; this is an inherent limitation of the method.

3.2 Fluorescence Microscopy

In order to record the response of GUVs to the introduction of JR2KC peptides, the vesicles needed to be immobilized. Immobilized GUV could be recorded both before and after JR2KC was introduced to the GUV. A method of immobilization by agarose gel was used for this purpose, and a protocol (protocol 2) was established. This protocol is presented in the results section as a brief, but still replicable description of the method. As protocol 1, it is meant to be an easily accessible set of instructions. Experimental details can be found in section 2.2.2

Protocol 2: GUV immobilization for fluorescence microscopy

This protocol describes a method for immobilizing GUVs without altering physical properties, based on the article *'Posing for a picture: vesicle immobilization in agarose gel'* (Lira *et al.*, 2016). By utilizing this method GUVs are suspended in a gel which prevents them from moving during microscopy, making finding and imaging suitable GUVs a more reliable process. Immobilization enables imaging of specific GUVs before and after the addition of an external substance into the gel, allowing for investigation of the effects of membrane-interacting molecules.

1) Dissolve powdered agarose with low gelling temperature (2-Hydroxyethyl agarose) in the same solution GUVs of interest are suspended in (e.g. PBS) to a concentration of 1% w/v. Portion the agarose into batches of a few hundred microliters, or however much is appropriate for the size of the observation chamber. These portions can be stored in a refrigerator.
2) Prepare an observation chamber and decide on what volume of suspended GUVs is desirable. During this project a 96-well plate with opaque black walls and transparent bottom was used as observation chamber, and 50 µl of total solution (agarose + GUV suspension) was used per well. Fill wells with half of that volume of GUV suspension, which may be diluted if desirable during this step.
3) Heat portions of 1% w/v agarose in a water bath above 65 °C (the gel's melting temperature) for a few minutes, until it is liquid. Place the portions in another water bath; the agarose has a gelling temperature of 26-30 °C, so the second water bath should be slightly warmer, about 40-50 °C. After a few minutes mix an equal volume of agarose with GUV suspension in the wells by pipetting up and down. The final concentration of agarose in the well should be 0.5% w/v. Let the solution cool before observing in microscope.

It should be noted that this immobilization was not able to fully immobilize vesicles when a liquid solution was added to the gel. In each of the time-lapses and images of figures 3-7, B3-19, but not figure 8, GUVs were suspended in 50 µl 0.5% (w/v) agarose gel with PBS, pH 7.36, as the liquid constituent. When 5 µl of a solution (peptide or LCO mixed with peptide in Milli-Q water) was added on top of the gel, GUVs which appeared immobile and focused in the microscope could be slightly displaced, so positioning and focus of the microscope needed to be adjusted periodically during time-lapse recordings after additions. Because of this some images taken during time-lapse recordings may be slightly out of focus, or the GUV may appear to have moved from one image to another. These experiments were performed in the wells of a 96-well plate with transparent bottom and black opaque walls, peptides and/or LCOs were only added once to a well.

In figures 3 and 4, as well as figures B3-B5 in appendix B small aliquots of JR2KC labelled with Cy5 was added to immobilized GUVs during time-lapse recordings of individual GUV. When added to GUVs with the composition 64.5:5:0.5:30 [POPC:MPB-PE:Liss-Rhod-PE:Chol] an apparent restructuring of the lipid membrane would often take place. As seen in figures 3 and B3-B5 the overall fluorescence intensity of these GUVs appears to diminish very slightly, and small, bright "dots" appear after a few seconds to a minute. These dots indicate phases of concentrated Liss-Rhod-PE in the lipid membrane. It should be noted that this apparent phase separation did not always occur when peptides were added, seen in figure B8. The reasons behind this are discussed in section 4.2.1. The total lipid concentration of GUVs in each well was estimated to be 30 µM at most, and peptide concentration in the well after addition was 1 µM.

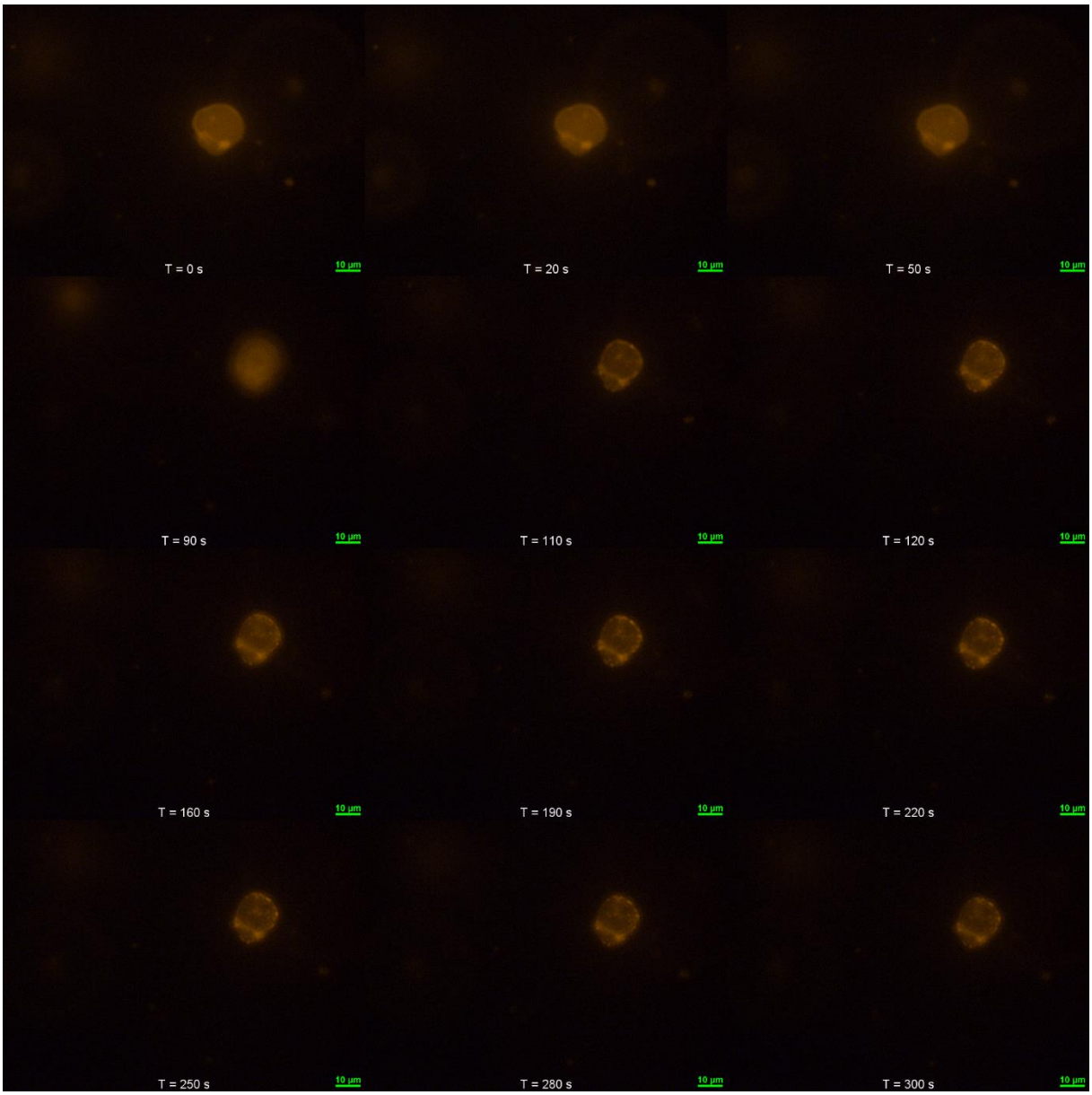

Figure 3. Time-lapse of a 30% Chol GUV. JR2KC-Cy5 were added around 60 seconds into the recording. The time-lapse was recorded as one image every 10 seconds for 5 minutes. GUV: 64.5:5:0.5:30 [POPC:MPB-PE:Liss-Rhod-PE:Chol], Filter: TRITC, Magnification: 60x, Exposure: 1 s, Analog gain: 4x, Shutter ND: 1.

In figure 4 JR2KC-Cy5 was added to 94.5:5:0.5 [POPC:MPB-PE:Liss-Rhod-PE] GUVs, that is without cholesterol. Although some change in membrane shape occurred, no dots as in the 30% cholesterol GUVs were observed. Some changes in membrane shape were observed, which was also the case for most GUVs after peptide addition.

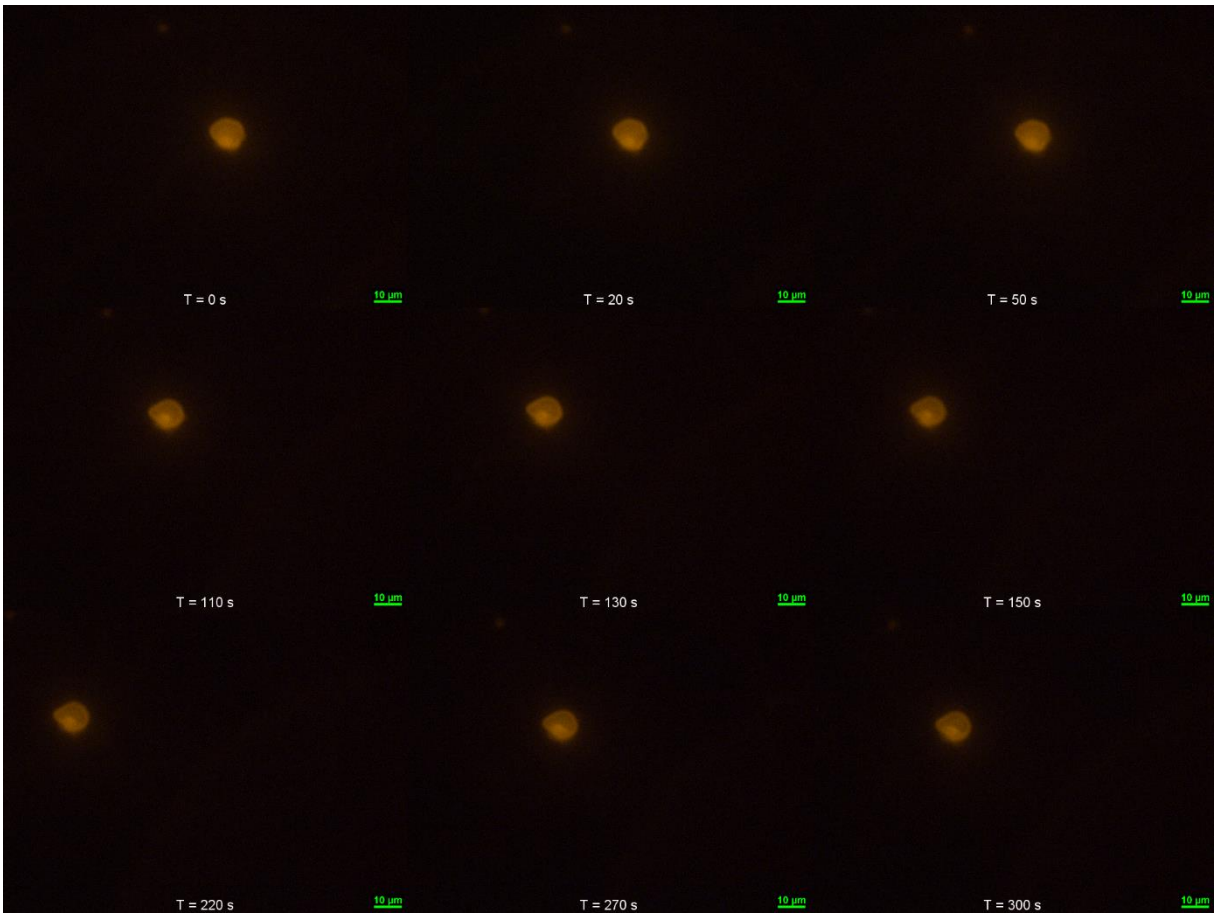

Figure 4. Time-lapse of a GUV without Chol. JR2KC-Cy5 were added around 60 seconds into the recording. The time-lapse was recorded as one image every 10 seconds for 5 minutes. GUV: 94.5:5:0.5 [POPC:MPB-PE:Liss-Rhod-PE], Filter: TRITC, Magnification: 60x, Exposure: 1 s, Analog gain: 4x, Shutter ND: 1.

As a control for the observed membrane changes JR2K was introduced to GUVs in the same manner as JR2KC. Figures 5, B7 and B8 depict time-lapses taken for this interaction. In these

studies no membrane phase changes were visible in neither 64.5:5:0.5:30 [POPC:MPB-PE:Liss-Rhod-PE:Chol] GUVs or 94.5:5:0.5 [POPC:MPB-PE:Liss-Rhod-PE] GUVs. Membrane shape changes were observed again, prominently in figure 5. These morphological changes could be induced by perturbations caused by adding fluid into the gel, or the GUV in figure 5 could have rotated inside the gel. The total lipid concentration of GUVs in each well was estimated to be 30 µM at most, and peptide concentration in the well after addition was 1 µM.

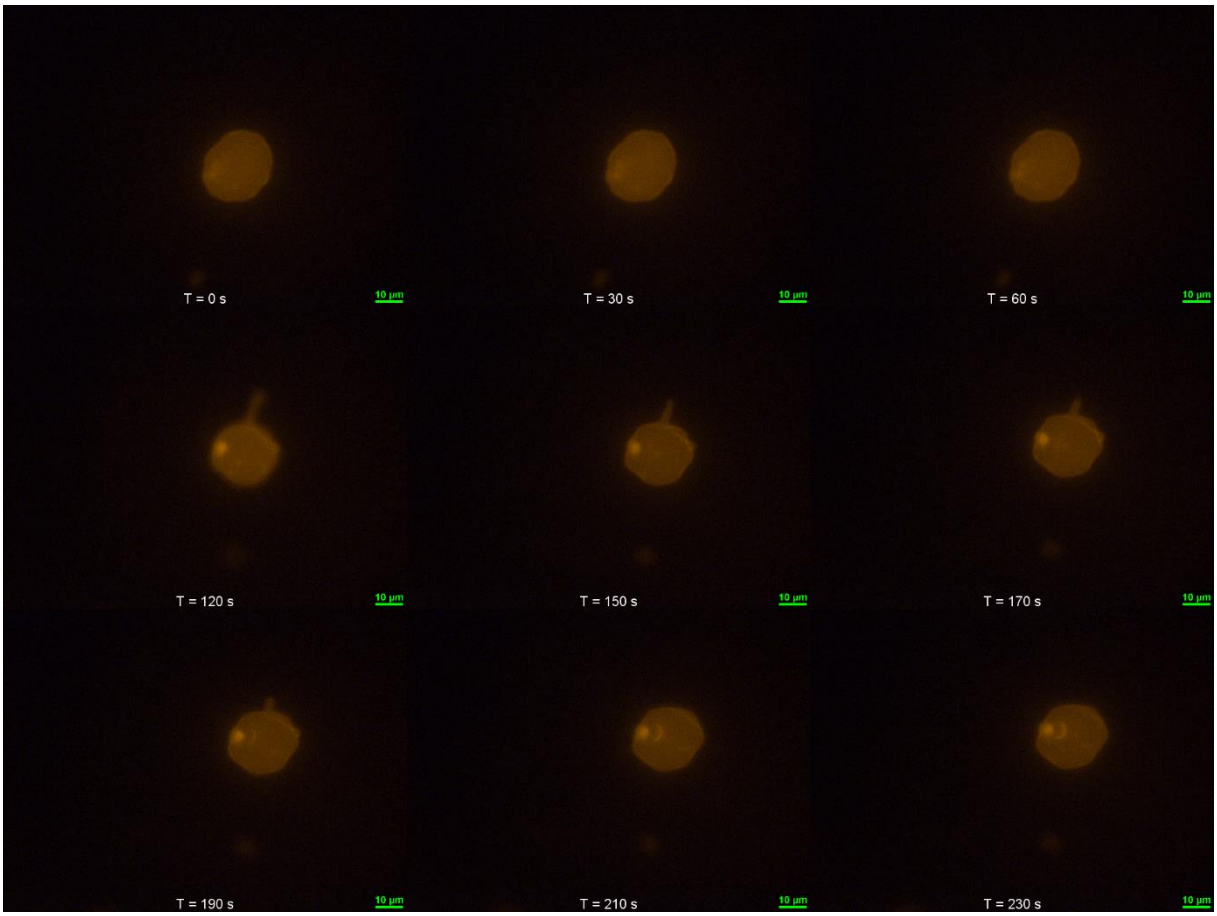

Figure 5. Time-lapse of a 30% Chol GUV. JR2K were added around 80 seconds into the recording. The time-lapse was recorded as one image every 10 seconds for 5 minutes. GUV: 64.5:5:0.5:30 [POPC:MPB-PE:Liss-Rhod-PE:Chol], Filter: TRITC, Magnification: 60x, Exposure: 1 s, Analog gain: 4x, Shutter ND: 1.

To study inhibition of JR2KC by pFTAA, 1:1 [JR2KC-Cy5:pFTAA] and 1:20 [JR2KC-Cy5:pFTAA] mixtures were introduced to immobilized GUV. In figure B8 no apparent phase change was induced to 64.5:5:0.5:30 [POPC:MPB-PE:Liss-Rhod-PE:Chol] GUVs, however

figures 6 and B9 depict formation of dots in the membrane similar to figures 3 and B3-B5 in presence of 1:1 [JR2KC-Cy5:pFTAA]. When 1:1 [JR2KC-Cy5:pFTAA] was added to 94.5:5:0.5 [POPC:MPB-PE:Liss-Rhod-PE] GUVs no phase changes could be observed (figure B10.). Before and after addition of JR2KC-Cy5 and pFTAA 1:1 mixture, images with 20x magnification were taken using Aqua Longpass to observe pFTAA fluorescence. The background before addition is shown in figure B11 and after in figure B12. When 1:20 [JR2KC-Cy5:pFTAA] was introduced to either 64.5:5:0.5:30 [POPC:MPB-PE:Liss-Rhod-PE:Chol] GUVs or 94.5:5:0.5 [POPC:MPB-PE:Liss-Rhod-PE] GUVs, no phase change was observed (figures B13-B15). No background image of pFTAA fluorescence was taken in this case, because the brightness might damage the camera. Even after 24 hours no phase changes could be observed; in figure B16 a GUV from the same well as figure B14 is shown 24 h after 1:20 [JR2KC-Cy5:pFTAA] was added. The total lipid concentration of GUVs in each well was estimated to be 30 µM at most, and peptide concentration in the well after addition was 1 µM. For 1:1 [JR2KC-Cy5:pFTAA] the LCO concentration in the well after addition was 1 µM, and for 1:20 [JR2KC-Cy5:pFTAA] the LCO concentration in the well after addition was 20 µM.

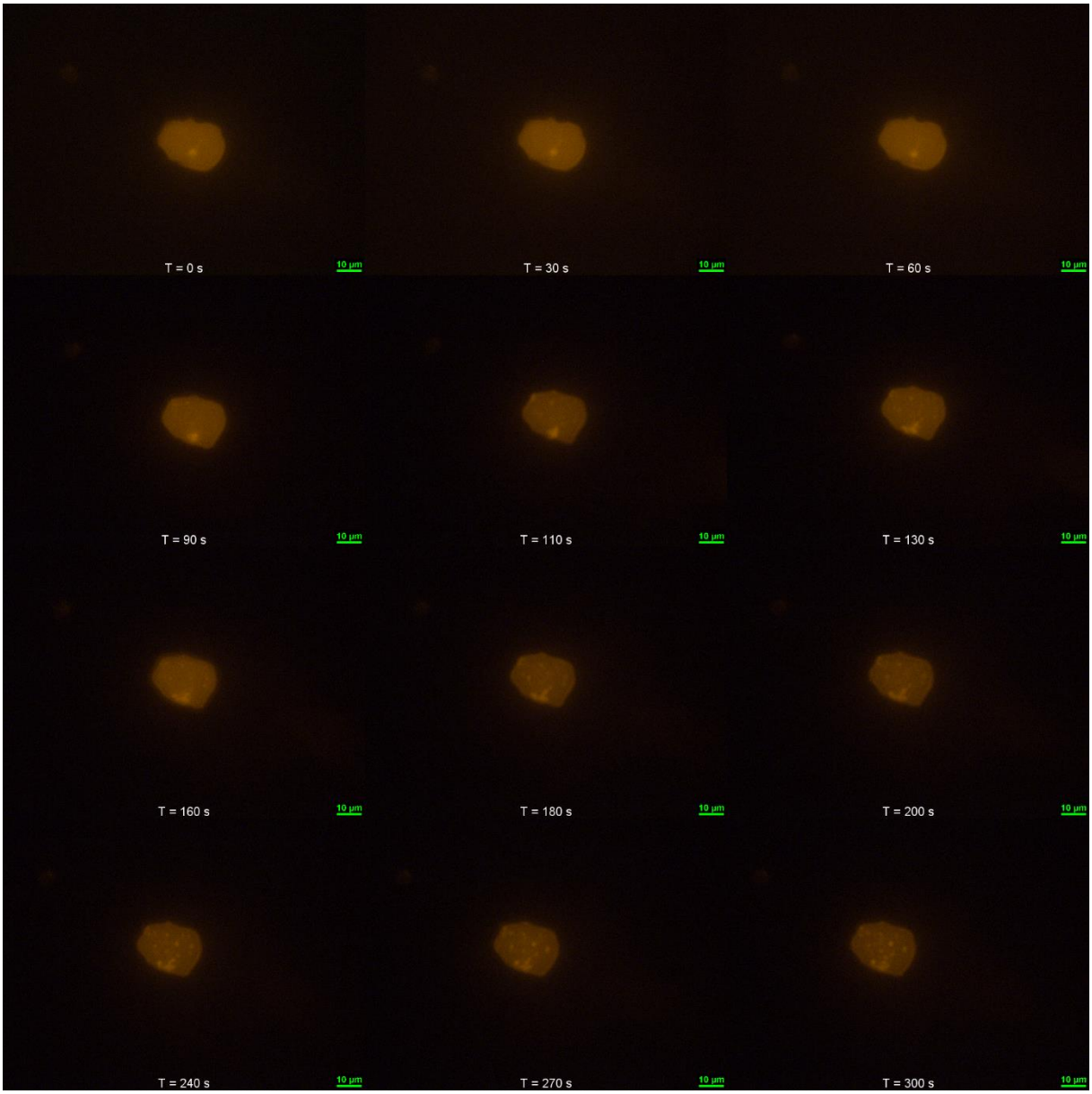

Figure 6. Time-lapse of a 30% Chol GUV. 1:1 [JR2KC-Cy5:pFTAA] mixture was added around 70 seconds into the recording. The time-lapse was recorded as one image every 10 seconds for 5 minutes. GUV: 64.5:5:0.5:30 [POPC:MPB-PE:Liss-Rhod-PE:Chol], Filter: TRITC, Magnification: 60x, Exposure: 1 s, Analog gain: 4x, Shutter ND: 1.

Attempts were made to study GUVs containing pFTAA-Chol as a fluorophore instead of Liss-Rhod-PE. The idea was that pFTAA bound directly to the membrane may be able to inhibit JR2KC at the membrane itself. However these were bleached too quickly for JR2KC-interaction time-lapses to be recorded. Figure B17 depicts complete bleaching by 2:10 min. Even with shutter neutral density (ND) 4 (which decreases excitation intensity by 4 times) as in figure 7, the image becomes unintelligible by 2:20 min. Attempts to use even higher ND

filters failed because the images were not bright enough to clearly see the liposomes clearly even from the start of the recordings. In this case a filter cube known as Aqua Longpass was used in order to observe fluorescence from pFTAA.

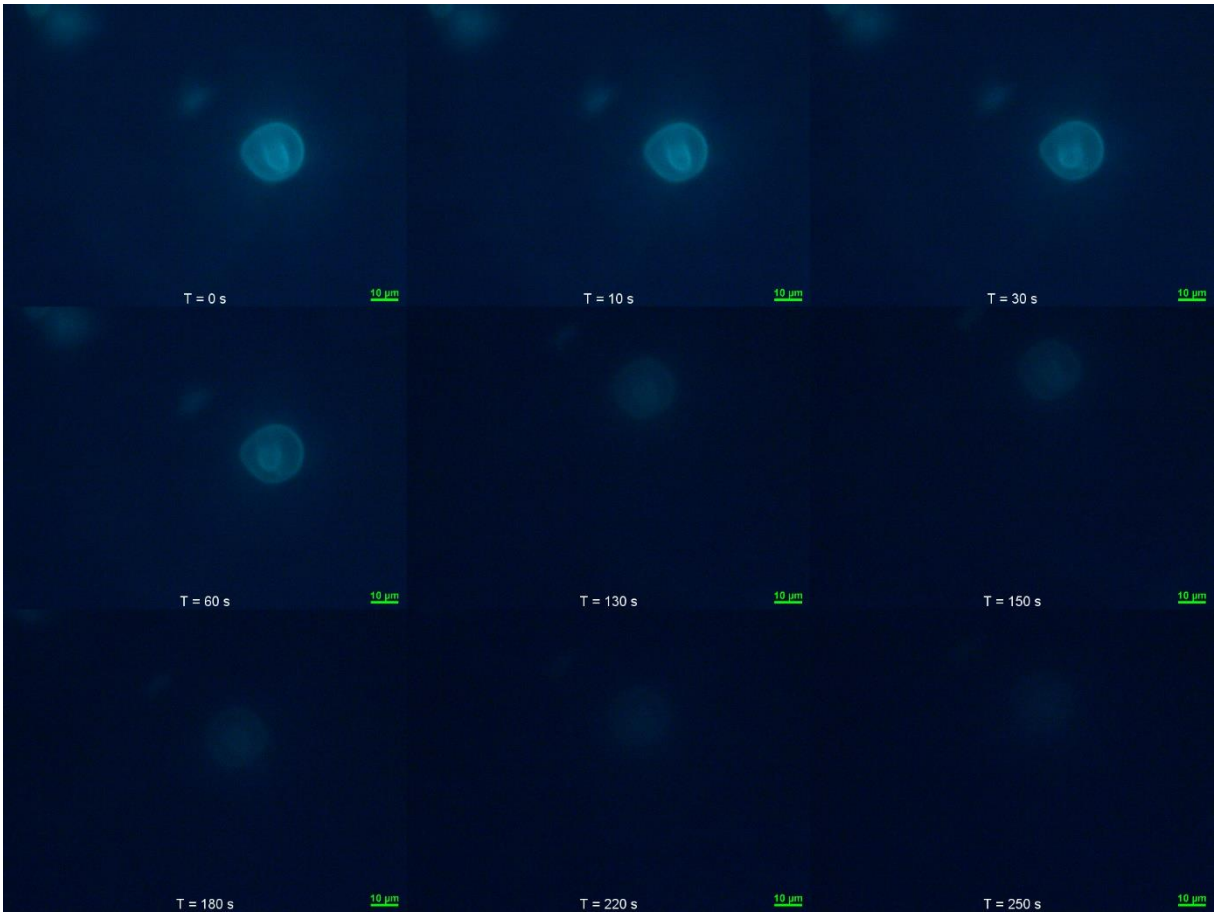

Figure 7. Time-lapse of a GUV containing Chol and pFTAA-Chol. JR2KC-Cy5 were added around 80 seconds into the recording. The time-lapse was recorded as one image every 10 seconds for 5 minutes. GUV: 65:5:29.5:0.5 [POPC:MPB-PE:Chol:pFTAA-Chol], Filter: Aqua Longpass, Magnification: 60x, Exposure: 4 s, Analog gain: 4x, Shutter ND: 4.

Since JR2KC had been labeled with Cy5, a Cy5 filter cube for the fluorescent microscope was utilized to observe Cy5 fluorescence at the GUV membrane. Such fluorescence had not been observable other than some background light in the experiments previously presented. It was thought that this could be due to quenching, so lower concentrations of JR2KC-Cy5 were tested. This would additionally give an idea of which proportions of JR2KC-Cy5 to MPB-PE were required for phase separation. 64.5:5:0.5:30 [POPC:MPB-PE:Liss-Rhod-PE:Chol] GUVs were tested with concentrations of JR2KC present corresponding to 1:0.8, 1:4, 1:8, 1:12 and 1:16

[JR2KC-Cy5: Available MPB-PE]. After 30 min incubation no phase change indicators such as the characteristic “dots” could be observed in the GUV with 1:20 [JR2KC-Cy5: Available MPB-PE]. In wells with 1:0.8 through 1:12 [JR2KC-Cy5: Available MPB-PE] some indicators of phase transition occurred. In figure 8 a liposome of the 1:12 [JR2KC-Cy5: Available MPB-PE] mixture is depicted, and a prominent ‘dot’ can be seen in the middle of the liposome, indicating a possible lipid raft. The GUVs were not immobilized for this so no time-lapses were recorded; figure 8 shows a free-flowing vesicle. Cy5 could not be visualized on GUVs using any of these concentrations of JR2KC-Cy5. The total lipid concentration of GUVs in each well was estimated to be 24 µM at most. Peptide concentration in the well after addition was 0.745 µM for 1:0.8 [JR2KC-Cy5: Available MPB-PE], 0.149 µM for 1:4 [JR2KC-Cy5: Available MPB-PE], 0.075 µM for 1:8 [JR2KC-Cy5: Available MPB-PE], 0.050 µM for 1:12 [JR2KC-Cy5: Available MPB-PE], and 0.037 µM for 1:16 [JR2KC-Cy5: Available MPB-PE].

Figure 8. Image of a 30% Chol GUV incubated with JR2KC proportional to MPB-PE in GUV membrane at 1:12 [JR2KC:MPB-PE] for 30 min. GUV: 64.5:5:0.5:30 [POPC:MPB-PE:Liss-Rhod-PE:Chol], Filter: Aqua Longpass, Magnification: 60x, Exposure: 1 s, Analog gain: 4x, Shutter ND: 1.

4. Discussion

In this section the results presented in section 3 will be discussed and analyzed. Societal impact and ethical implications of the work will also be presented here. A reflection on the process is written in appendix A.

4.1 GUV preparation

The final version of the GUV preparation protocol (Protocol 1) is a protocol that will reliably generate usable GUVs. Due to the fundamental nature of swelling liposomes from dried membranes, aggregates and multilamellar vesicles (MLV) will always be produced by this protocol (Reeves and Dowben, 1969), but in each sample studied one could always find GUVs. The protocol readily usable due to its use of mostly standard laboratory equipment. Some unusual equipment is required: syringes capable of working with organic solvents such as chloroform (Hamilton syringes) but a lab working with lipids and other chemicals dissolved in organic solvent should be equipped with such, PTFE sheets are a common material used in for example pipe coating and packings and can be acquired from manufacturers of plastics. A method based on fluid interfaces could be developed, provided the desired lipids are dissolvable in oils such as mineral oil. For example a microfluidics based approach is a fairy common way of introducing lipids dissolved in oil to aqueous solution, and having GUVs bud from the interface (Dimova and Marques, 2019). To develop such a method, experience working with emulsions and microfluidics would be required. Protocol 1 has been tested successfully by one person other than the author of this report.

As noted in appendix A (process section of the report) the use of water saturated nitrogen to rehydrate lipid films opened up the possibility of including only 5 mol% charged lipids (MPB-PE) in the membrane composition. It also allowed for a day's shorter preparation time than at the start of the project, and the time required is now approximately one workday and a couple of hours the day after. Overall the protocol has become quite manageable and should be easily accessible to new users. The method for generating water saturated nitrogen, explained in section 3.1 and shown in figure 1 is somewhat improvised though effective. Water saturated nitrogen gas has been used to rehydrate lipid films in several papers (Reeves and Dowben, 1969; Akashi *et al.*, 1996, 1998) but the method for generating it was not explained. No such method was found in research, but the method shown here could be improved with specialized equipment. A more efficient heating element could speed up the process of heating water, and a rehydration chamber with optimized N_2 flow could increase lipid film protection from oxygen

and decrease time spent significantly; Akashi et al. (1998) only needed one minute to rehydrate films, but did not describe how this was accomplished. If there are dedicated instruments for generating water saturated gases, such an instrument may be preferable to the setup used in this project. One thing to consider for improvement is the cooling rate of the solution after overnight swelling but before the GUVs are harvested. The cooling rate can influence the natural face separation of the GUVs (Morales-Penningston *et al.*, 2010) and can also impact GUV aggregate yield before harvesting (Kubsch *et al.*, 2017).

4.2 Fluorescence microscopy

As with all methods of GUV production to be able to differentiate GUV from other lipid structures in the solution, a "critical eye" (Dimova and Marques, 2019) is needed. This is developed with experience over time observing vesicle solutions. One of the key characteristics to learn to look for is brightness, which can help separate GUV from MLV. If fluorescent probes are embedded int the membrane (as is the case for MPB-PE) the multiple membranes contained in MLV will all have fluorescent probes dispersed in them. By comparing the brightness of vesicles in the solution, one can determine that the vesicles with lowest fluorescence intensity should be unilamellar, although there is no way to be entirely certain.

4.2.1 Analysis of microscopy results.

Formation of 'dots' during JR2KC addition to GUVs containing 30 mol% cholesterol (64.5:5:0.5:30 [POPC:MPB-PE:Liss-Rhod-PE:Chol]) is a probable sign pointing towards the formation of lipid rafts around JR2KC binding into the membrane, or at least that a phase separation occurs. MPB-PE, which binds JR2KC via a maleimide moiety to thiol on the peptide, and the fluorophore Liss-Rhod-PE have the same non-polar fatty acid moieties, and presumably partition mostly into the same phase since probe partition relies on chemical environment more than membrane phase (Bagatolli, 2006). If such a phenomenon occurs, then the dots appearing on the membrane would indicate higher localized concentrations of Liss-Rhod-PE, and thus also higher concentrations of MPB-PE in those phases, some of which would be bound to JR2KC-Cy5. These local concentrations could thus be the hypothesized lipid rafts. This is also supported by the JR2K control experiments, where no phase separation was observed in GUV containing 30 mol% cholesterol, meaning that the peptide has to bind in order for phase separation to occur. As noted in section 3.2 however, sometimes no phase separation would occur after addition of Jr2KC-Cy5. A possible explanation is that spreading out and drying a lipid film in the GUV preparation creates non-uniform lipid membranes, meaning that some GUVs will contain more or less proportionally of the various lipid components (Dimova and

Marques, 2019). It could be that some GUVs containing cholesterol had a too small proportion of cholesterol or MPB-PE to generate phase separation. Since JR2KC will rapidly permeabilize the lipid membrane when bound (Lim *et al.*, 2016) the lipid raft hypothesis seems more likely to be true as lipid rafts often occur naturally, coalescing around membrane partitioning proteins and often creating clusters of such proteins (Simons and Ikonen, 1997). Other data supporting the hypothesis is that JR2KC did not cause phase separation in GUVs containing no cholesterol (94.5:5:0.5 [POPC:MPB-PE:Liss-Rhod-PE]), showing that a phase change at least is involved in the increased release rate of the system when 30 mol% cholesterol is incorporated. Unfortunately, we were unable to visualize JR2KC directly binding to the GUVs via Cy5 dye bound to JR2KC. When observing GUVs after peptide addition using a Cy5 filter only a slight background light could be seen in the eyepiece, too faint to be distinguishable in images. Whether quenching was causing this was checked by decreasing JR2KC concentration as in figure 8, but Cy5 could not be visualized even at lower concentrations. Overall the hypothesis that JR2KC binding to liposomes with the composition 65:5:30 [POPC:MPB-PE:Chol] induces phase separation into lipid rafts, causing increase in release efficiency from the liposomes, is highly supported by the results.

When introduced to GUVs along JR2KC, it is clear from the difference between 1:1 and 1:20 [JR2KC:pFTAA] mixtures that the LCO pFTAA could inhibit JR2KC binding to GUV. That this inhibition did not occur, or at least was not as effective, when the mixture was 1:1 but did with an overwhelming amount of 20 times the JR2KC suggests that the inhibition is competitive between MPB-PE binding and pFTAA interaction. As seen in figure B16 the inhibition could persist for 24 h, or it may have lasted long enough for the thiol groups to oxidize, thus preventing GUV binding. Comparing figures B11 and B12 it seems that pFTAA is strongly fluorescent in solution, and no binding to the GUV along with the peptide could be observed. Unfortunately the GUVs containing pFTAA-Chol (65:5:29.5:0.5 [POPC:MPB-PE:Chol:pFTAA-Chol]) were photobleached to rapidly to record time lapses of, so it is yet to be determine whether phase separation would occur in such GUV, or if pFTAA-Chol would bind and inhibit JR2KC. Although considering the phase separation in 1:1 [JR2KC:pFTAA] it seems likely that pFTAA does not inhibit JR2KC when it has embedded into a GUV, and that pFTAA is always dissolved in the solution.

4.2.2 Continuing discussion on fluorescence microscopy.

To further characterize the GUV interactions with peptides and LCOs, using more sensitive microscopy techniques is a natural first step. A common variant of this is laser scanning

confocal microscopy, or confocal microscopy for short. Confocal microscopy is a form of inverted fluorescence microscopy that has often been used when studying fluorescently labelled cells, and is also often used with GUV since they are generally cell sized (Bagatolli, 2006; Shimokawa *et al.*, 2010; Wheeler and Tyler, 2011; Kubsch *et al.*, 2017). This technique offers a substantial advantage over wide-field fluorescence microscopy for the purposes of further studies of the liposome-JR2KC interactions. Confocal microscopy takes a stack of vertical image slices of an object of study and digitally generates three-dimensional models of the object, while preserving fluorescence intensity and color in each pixel. This is particularly useful with respect to studies of the lipid-raft hypothesis, as it could visualize the entire membrane structure in one model. Being able to do so would make it easier to identify patterns of lipid rafts in the membrane, and to study the formation of hypothesized rafts in time-lapses. With increased sensitivity, it may also be possible to detect Cy5 fluorescence using confocal microscopy.

However, an even better technique to consider would be laser scanning two-photon excitation fluorescence microscopy, more commonly named two-photon microscopy. This technique can generate three-dimensional models in the same manner as confocal microscopy, but with the key advantage of causing less photobleaching to the fluorophores (Bagatolli, 2006; Wheeler and Tyler, 2011; Dimova and Marques, 2019). Employing two-photon microscopy could eliminate the problem of photobleaching when studying GUV containing pFTAA-Chol as fluorophore. Moreover, the fluorescent probe Laurdan could be used to further characterize phase separation in the liposomes. Laurdan is a fluorophore for which emission spectra shits in the presence of water molecules due to dipolar relaxation. When embedded in a lipid membrane Laurdan will because of this phenomena emit with different emission maxima depending on the permeability of water in the membrane, which depends on the phase state of membranes (Parasassi *et al.*, 1990). This has been confirmed to be true even for membranes containing cholesterol (Parasassi *et al.*, 1994). Laurdan can thus be distinguishable in systems with separated phases, and can be used to visualize phase separation with two-photon microscopy (Bagatolli, Parasassi and Gratton, 2000). When working with Laurdan a generalized polarization (GP) value is calculated as $GP = \frac{I_B - I_R}{I_B + I_R}$, where I_B is the blue shifted emission peak (440 nm) of Laurdan and I_R is the red shifted emission peak (490 nm) of Laurdan (Parasassi *et al.*, 1990; Dimova and Marques, 2019). As mentioned earlier two-photon and confocal microscopy can record fluorescence intensity data for each pixel in their imaging, and a GP spectrum model can be calculated by applying the GP formula to models

generated by the microscopy (Bagatolli, 2006; Shimokawa *et al.*, 2010; Kubsch *et al.*, 2017). GP spectrum model could also be compared with other fluorescence probes, such as Liss-Rhod-PE to correlate membrane phases with Liss-Rhod-PE partition in different phases, especially if Laurdan could be used in the same GUVs as the other probe. With the right equipment this can be performed by confocal microscopy despite it being more prone to photobleaching than two-photon microscopy (Bagatolli, 2006). Even widefield fluorescence microscopy has been used for lipid membrane imaging with Laurdan, although it required special equipment in the form of a three-channel emission splitter for the microscope, and extensive experience in fluorescence microscopy (Wheeler and Tyler, 2011).

For the future prospects of what has been studied in this project there are two main conclusions: First is that while inhibition of JR2KC by pFTAA is interesting, it is probably not useful to study by the methods devised in this project. The fluorescence is too sensitive to photobleaching for the instruments used in this case, and inhibition of peptide by the LCO in solution rather than at the membrane means that GUV won't be useful in visualization by microscopy. Second, that lipid raft formation could be further studied with the aim of implementation in a drug delivery system. As explained in the introduction (section 1.), the project that resulted in this master's thesis was commissioned in order to aid development of a drug delivery system using liposomes composed mainly of POPC and MPB-PE as the drug delivery vehicle and JR2KC as a drug release activator. Inclusion of 30 mol% cholesterol was investigated with fluorescence microscopy for visual evidence of possible lipid raft formation when JR2KC binds to the liposome surface, as an increase in release rate from liposomes was previously detected. Microscopy studies in this project indicated that lipid raft formation occurred, and now this phenomenon needs to be further studied and developed. The protocols presented in this report may be useful in order to further hone the lipid raft formation and optimize it for the future drug delivery system. Observation of lipid raft formation on GUVs will still be essential for the development of the LUV-based drug delivery system.

4.2 Ethics statement and societal aspects

In the case of this project every chemical component is completely synthetic; including lipids, LCOs, peptides and other materials. The only non-synthetic material used is cholesterol, which is plant derived and thus not a great ethical concern. No living or dead cells were used during any stage of this project.

The potential use of the liposome-JR2KC system investigated during this project for cancer treatment is of great interest to the future of cancer therapy. Should this project contribute to the formulation of a fully useable drug-delivery system targeting cancer tissues then it could be considered to have a positive societal impact. Drug delivery systems allow for more targeted doses of pharmaceuticals to specific tissues. The intention of this drug delivery system is to generate a rapid release of anticancer drugs by liposome carriers in the presence of cancer tissue. Doing this limits the exposure to harmful drugs for healthy tissues in the body, and potentially for smaller overall doses to be used given drug release only occurs at the cancer tissue. In this great potential for healthcare the ethical and societal justification for the undertaking of this project can be found, if healthcare needs justification.

Acknowledgements

I would like to thank my supervisors Johanna Utterström and Robert Selegård and my examiner Daniel Aili for helping me with and contributing to this project. Thank you to Tomas Ederth for showing me how to use his TIRF microscope. I would also like to thank everyone else at the laboratory of molecular materials as well as my fellow masters students Livia Civitelli and Philip Lifwergren for being lovely to work with and always supportive.

References

Akashi, K.-I. *et al.* (1996) 'Preparation of giant liposomes in physiological conditions and their characterization under an optical microscope', *Biophysical Journal*, 71(6), pp. 3242–3250. doi: 10.1016/S0006-3495(96)79517-6.

Akashi, K. *et al.* (1998) 'Formation of Giant Liposomes Promoted by Divalent Cations: Critical Role of Electrostatic Repulsion', *Biophysical Journal*, 74(6), pp. 2973–2982. doi: 10.1016/S0006-3495(98)78004-X.

Bagatolli, L. A. (2006) 'To see or not to see: Lateral organization of biological membranes and fluorescence microscopy', *Biochimica et Biophysica Acta - Biomembranes*. doi: 10.1016/j.bbamem.2006.05.019.

Bagatolli, L. A., Parasassi, T. and Gratton, E. (2000) 'Giant phospholipid vesicles: Comparison among the whole lipid sample characteristics using different preparation methods - A two photon fluorescence microscopy study', *Chemistry and Physics of Lipids*. doi: 10.1016/S0009-3084(00)00118-3.

Bozzuto, G. and Molinari, A. (2015) 'Liposomes as nanomedical devices', *International journal of nanomedicine*. Dove Medical Press, 10, pp. 975–999. doi: 10.2147/IJN.S68861.

Civitelli, L. *et al.* (2016) 'The Luminescent Oligothiophene p-FTAA Converts Toxic A □ 1 – 42 Species into Nontoxic Amyloid Fibers with Altered', 291(17), pp. 9233–9243. doi: 10.1074/jbc.M115.696229.

Dao, T. P. T. *et al.* (2017) 'Membrane properties of giant polymer and lipid vesicles obtained by electroformation and pva gel-assisted hydration methods', *Colloids and Surfaces A: Physicochemical and Engineering Aspects*. doi: 10.1016/j.colsurfa.2017.09.005.

Dimova, R. (Ed. . and Marques, C. M. (Ed. . (2019) *The Giant Vesicle Book., CRC Press*. Boca Raton: CRC Press. doi: 10.1201/9781315152516.

Jain, K. K. (2020) 'An Overview of Drug Delivery Systems BT - Drug Delivery Systems', in Jain, K. K. (ed.). New York, NY: Springer New York, pp. 1–54. doi: 10.1007/978-1-4939-9798-5_1.

De Jong, O. G. *et al.* (2019) 'Drug Delivery with Extracellular Vesicles: From Imagination to Innovation', *Accounts of Chemical Research*, 52(7), pp. 1761–1770. doi: 10.1021/acs.accounts.9b00109.

Kubsch, B. *et al.* (2017) 'Phase behavior of charged vesicles under symmetric and asymmetric solution conditions monitored with fluorescence microscopy', *Journal of Visualized Experiments*, 2017(128), pp. 1–17. doi: 10.3791/56034.

Levental, I. and Veatch, S. L. (2016) 'The Continuing Mystery of Lipid Rafts', *Journal of Molecular Biology*. doi: 10.1016/j.jmb.2016.08.022.

Lim, S. K. *et al.* (2016) 'Tuning Liposome Membrane Permeability by Competitive Peptide Dimerization and Partitioning-Folding Interactions Regulated by Proteolytic Activity', *Scientific Reports*. Nature Publishing Group, 6(October 2015), pp. 1–9. doi: 10.1038/srep21123.

Lira, R. B. *et al.* (2016) 'Posing for a picture : vesicle immobilization in agarose gel', *Nature Publishing Group*. Nature Publishing Group, (May), pp. 1–12. doi: 10.1038/srep25254.

Manley, S. and Gordon, V. D. (2008) 'Making giant unilamellar vesicles via hydration of a lipid film', *Current Protocols in Cell Biology*, (SUPPL. 40), pp. 1–13. doi: 10.1002/0471143030.cb2403s40.

Méléard, P. *et al.* (1997) 'Bending elasticities of model membranes: Influences of temperature and sterol content', *Biophysical Journal*, 72(6), pp. 2616–2629. doi: 10.1016/S0006-3495(97)78905-7.

Méléard, P., Bagatolli, L. A. and Pott, T. (2009) 'Giant Unilamellar Vesicle Electroformation. From Lipid Mixtures to Native Membranes Under Physiological Conditions', in *Methods in Enzymology*, pp. 161–176. doi: 10.1016/S0076-6879(09)65009-6.

Mora, N. L. *et al.* (2017) 'Evaluation of dextran(ethylene glycol) hydrogel films for giant unilamellar lipid vesicle production and their application for the encapsulation of polymersomes', *Soft Matter*. Royal Society of Chemistry, 13(33), pp. 5580–5588. doi: 10.1039/c7sm00551b.

Morales-Penningston, N. F. *et al.* (2010) 'GUV preparation and imaging: Minimizing artifacts', *Biochimica et Biophysica Acta - Biomembranes*. doi: 10.1016/j.bbamem.2010.03.011.

Parasassi, T. *et al.* (1990) 'Phase fluctuation in phospholipid membranes revealed by Laurdan fluorescence', *Biophysical Journal*. Elsevier, 57(6), pp. 1179–1186. doi: 10.1016/S0006-3495(90)82637-0.

Parasassi, T. *et al.* (1994) 'Influence of cholesterol on phospholipid bilayers phase domains as detected by Laurdan fluorescence', *Biophysical Journal*, 66(1), pp. 120–132. doi: https://doi.org/10.1016/S0006-3495(94)80763-5.

Pereno, V. *et al.* (2017) 'Electroformation of Giant Unilamellar Vesicles on Stainless Steel Electrodes', *ACS Omega*. American Chemical Society, 2(3), pp. 994–1002. doi: 10.1021/acsomega.6b00395.

Pott, T. and Philippe, M. (2008) 'Giant unilamellar vesicle formation under physiologically relevant conditions', 154, pp. 115–119. doi: 10.1016/j.chemphyslip.2008.03.008.

Reeves, J. P. and Dowben, R. M. (1969) 'Formation and properties of thin-walled phospholipid vesicles', *Journal of Cellular Physiology*. John Wiley & Sons, Ltd, 73(1), pp. 49–60. doi: 10.1002/jcp.1040730108.

Rydberg, J., Baltzer, L. and Sarojini, V. (2013) 'Intrinsically unstructured proteins by design—electrostatic interactions can control binding, folding, and function of a helix-loop-helix heterodimer', *Journal of Peptide Science*. John Wiley & Sons, Ltd, 19(8), pp. 461–469.

doi: 10.1002/psc.2520.

Sarmento, M. J., Prieto, M. and Fernandes, F. (2012) 'Reorganization of lipid domain distribution in giant unilamellar vesicles upon immobilization with different membrane tethers', *Biochimica et Biophysica Acta - Biomembranes*. Elsevier B.V., 1818(11), pp. 2605–2615. doi: 10.1016/j.bbamem.2012.05.028.

Shimokawa, N. *et al.* (2010) 'Phase separation of a mixture of charged and neutral lipids on a giant vesicle induced by small cations', *Chemical Physics Letters*. Elsevier B.V., 496(1–3), pp. 59–63. doi: 10.1016/j.cplett.2010.07.021.

Simons, K. and Ikonen, E. (1997) 'Functional rafts in cell membranes', *Nature*, 387(6633), pp. 569–572. doi: 10.1038/42408.

Skyttner, C. *et al.* (2018) 'Tuning Liposome Membrane Permeability by Competitive Coiled Coil Heterodimerization and Heterodimer Exchange', *Langmuir*. American Chemical Society, 34(22), pp. 6529–6537. doi: 10.1021/acs.langmuir.8b00592.

Skyttner, C. *et al.* (2019) 'Sequence and length optimization of membrane active coiled coils for triggered liposome release', *Biochimica et Biophysica Acta - Biomembranes*, 1861(2), pp. 449–456. doi: 10.1016/j.bbamem.2018.11.005.

Stein, H. *et al.* (2017) 'Production of isolated giant unilamellar vesicles under high salt concentrations', *Frontiers in Physiology*. Frontiers Research Foundation, 8(FEB). doi: 10.3389/fphys.2017.00063.

Steinkühler, J. *et al.* (2018) 'Charged giant unilamellar vesicles prepared by electroformation exhibit nanotubes and transbilayer lipid asymmetry', *Scientific Reports*, 8(1), pp. 1–9. doi: 10.1038/s41598-018-30286-z.

Szarvas, T. *et al.* (2010) 'Matrix metalloproteinase-7 as a marker of metastasis and predictor of poor survival in bladder cancer', *Cancer Science*, 101(5), pp. 1300–1308. doi: 10.1111/j.1349-7006.2010.01506.x.

Tsumoto, K. *et al.* (2009) 'Efficient formation of giant liposomes through the gentle hydration of phosphatidylcholine films doped with sugar', *Colloids and Surfaces B: Biointerfaces*, 68(1), pp. 98–105. doi: 10.1016/j.colsurfb.2008.09.023.

Veatch, S. L. and Keller, S. L. (2002) 'Organization in Lipid Membranes Containing Cholesterol', *Physical Review Letters*, 89(26), pp. 1–4. doi: 10.1103/PhysRevLett.89.268101.

Veatch, S. L. and Keller, S. L. (2003) 'Separation of Liquid Phases in Giant Vesicles of Ternary Mixtures of Phospholipids and Cholesterol', *Biophysical Journal*. Elsevier, 85(5), pp. 3074–3083. doi: 10.1016/S0006-3495(03)74726-2.

Weinberger, A. *et al.* (2013) 'Gel-assisted formation of giant unilamellar vesicles', *Biophysical Journal*. doi: 10.1016/j.bpj.2013.05.024.

Wheeler, G. and Tyler, K. M. (2011) 'Widefield microscopy for live imaging of lipid domains and membrane dynamics', *Biochimica et Biophysica Acta - Biomembranes*. doi: 10.1016/j.bbamem.2010.11.017.

Appendix A: Process

During the planning phase of the project a time plan was established, which is presented as a GANTT chart in table A1. Initial planning occurred during the first two project weeks and was presented during the third week in the form of a planning report and a presentation. The first milestone after this was to establish a protocol for GUV formation. Three main methods of GUV preparation were identified during planning as possible methods: Gentle hydration, electroformation, and gel-assisted swelling. Gentle hydration was identified as the most likely method to work due to it working well with charged lipids and in physiological conditions (Akashi *et al.*, 1996). Designs for an electroformation chamber were considered, but it was determined by further research that the problems caused by incorporating charged lipids in electroformation (Steinkühler *et al.*, 2018) were too great for the method to be viable. Gel assisted swelling is a method that has not been discussed previously in the main part of this report. This method entails swelling of a lipid film spread on top of a gel, which speeds up the flow of swelling fluid between bilayer deposits (Weinberger *et al.*, 2013). This can be done with several different gels (Mora *et al.*, 2017), but the method was eventually abandoned because of contaminations of its propensity to contaminate the GUV membrane (Dao *et al.*, 2017). Gentle hydration however saw immediate success.

Table A1. GANTT chart used in the planning of this project. Milestones (MS) marked with dots or stars. Time scheduled for an activity marked in yellow. Work planned to be performed way from the laboratory marked in magenta.

Project week	1	2	3	4	5	6	7	8	9	10	11	12	13	14	15	16	17	18	19	20	21	22
Calendar week	4	5	6	7	8	9	10	11	12	13	14	15	16	17	18	19	20	21	22	23	24	25
Activity																						
Planning																						
MS1: Planning report and presentation			•																			
Study: Electroformation																						
Study: Gel assisted swelling																						
Study: Gentle Hydration																						
Preparation FL microscopy																						
MS2: Protocols for GUV estblished									•													
Writing half-time report																						
MS3: Half-time seminar										•												
Study: Peptide-GUV																						
Study: Peptide-LCO																						
MS4: Peptide-GUV complete																	•					
MS5: Peptide-LCO complete																	•					
Writing report, feedback etc.																						

MS6: Report to opponent and examiner																			•			
MS7: Project presentation																					★	
MS8: Final corrected report																						★

The gentle hydration setup was based largely on the setups used by Kubsch et al. (2017) and Manley et al. (2008), where lipid films were spread on PTFE pads. At first a steam-based setup for rehydration was used, illustrated in figure A1, which was also used by Kubsch et al. (2017). In this setup the lipid films were rehydrated for 4-6 hours at 45 °C. This setup was initially successful when 10-20 mol% MPB-PE was incorporated, but not with 5 mol% as desired. This was predicted by literature to occur when using gentle hydration in physiological conditions such as PBS (Akashi *et al.*, 1996). During the weeks leading up to the half-time seminar milestone, various factors such as rehydration time, temperature, swelling time etc. were examined to optimize the GUV preparation. Eventually, the water-saturated nitrogen setup presented in the main part of this report was able to hydrate lipid films enough for GUVs containing 5 mol% MPB-PE to be consistently produced. Initially, a goal of the project was to produce GUVs of mainly POPC and a small portion of Liss-Rhod-PE as fluorescent label, as a control during fluorescence microscopy. This was later switched to use JR2K as a control for JR2KC, by introducing it to GUVs of the same compositions. However, 99.5:0.5 [POPC:Liss-Rhod-PE] GUVs were produced in PB buffer with added Ca^{2+} which bind to lipid head groups and induce enough charge repulsion to form GUVs with gentle hydration (Akashi *et al.*, 1998).

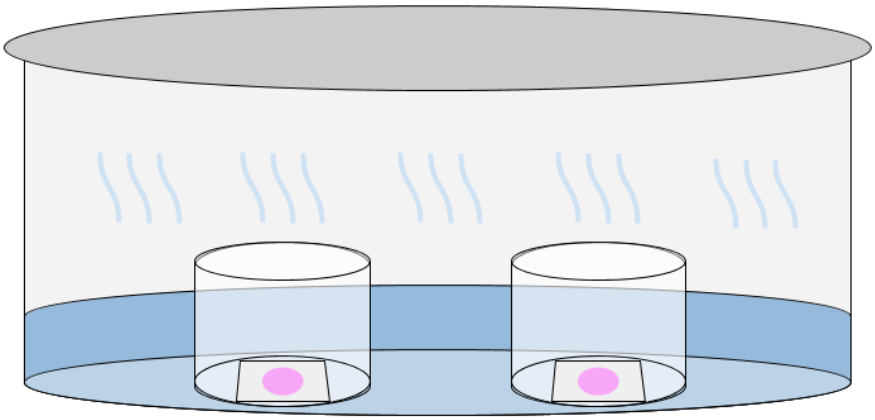

Figure A1. Setup for dried lipid film rehydration with steam. Beakers containing lipid film (pink) spread on PTFE pads are placed in a thin layer ow MilliQ water inside a sealed glass vessel. When placed in a heated oven, steam is generated and lipid films are rehydrated over a few hours.

By the half-time presentation, the third milestone of the planning schedule, GUV with compositions 64.5:5:0.5:30 [POPC:MPB-PE:Liss-Rhod-PE:Chol] and 94.5:5:0.5 [POPC:MPB-PE:Liss-Rhod-PE] had been successfully produced. Protocol 1 was written shortly after the half time seminar, but the methodology was established by the planned time in the 9th week of the project. After this point, JR2KC was labeled with Cy5. It became clear that GUVs needed to be immobilized in order to record JR2KC interactions with single GUV during time lapses. Fluorescence microscopy studies were pushed further in the schedule, and a protocol for immobilization, protocol 2, was established during project weeks 10-11. During this time it was discovered that pipette tips cut for GUV harvesting could contaminate samples with plastic pieces, strongly visible in fluorescence microscopy. Because of this a recommendation to was cut pipette tips before harvesting was added to protocol 1. An absence from the lab was planned during project weeks 12-13 (magenta in table A1), however this was cancelled, and fluorescence microscopy observations were started during this time. For the rest of the project time the results presented in this report were gathered and the report was written in accordance to time allotted in table A1.

Appendix B: Supplementary Images

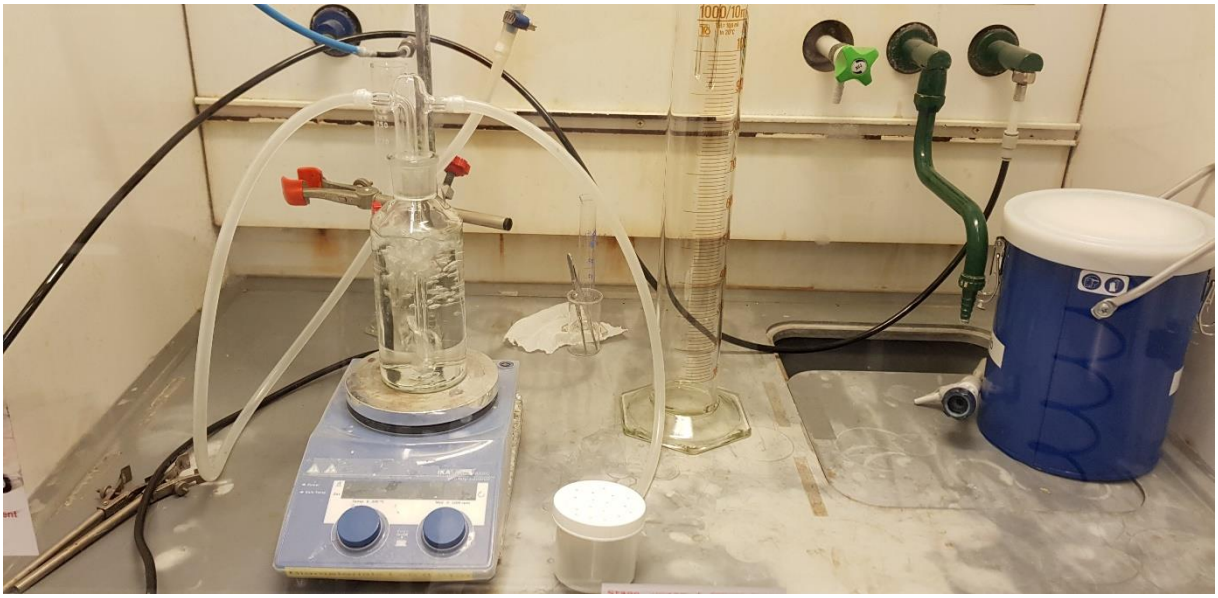

Figure B1. Setup for rehydration using water saturated N_2. N_2 is bubbled into heated MilliQ water through the tube to the left of the glass bottle, and the vapors are directed through the other tube into a chamber where lipid films are rehydrated.

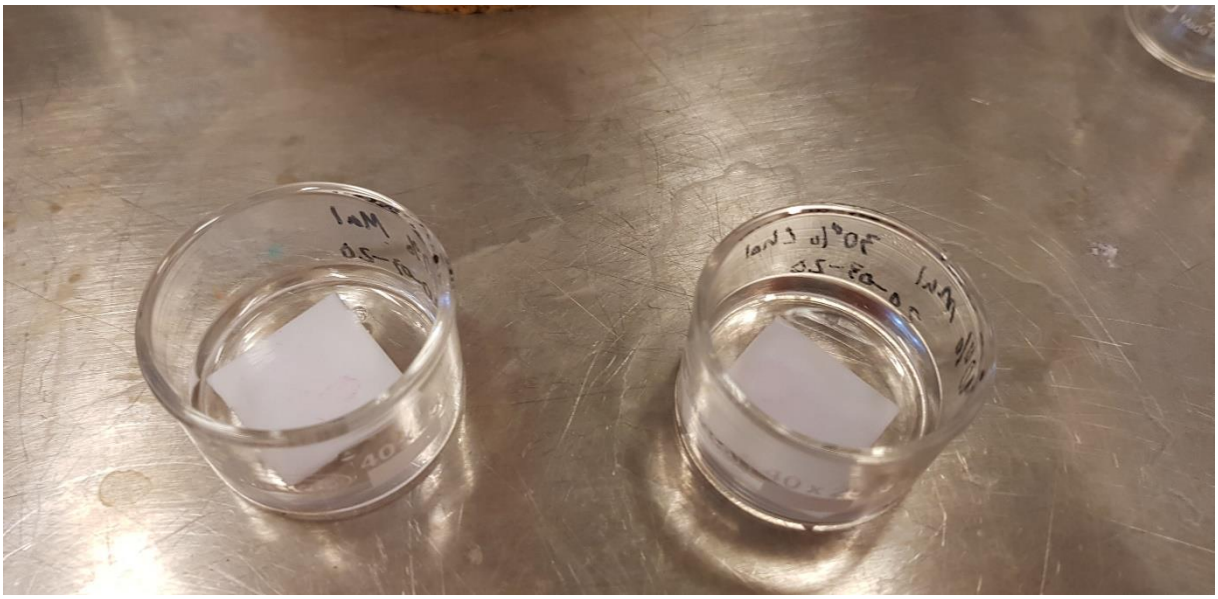

Figure B2. PTFE pads placed in beakers, submerged in 5 ml PBS.

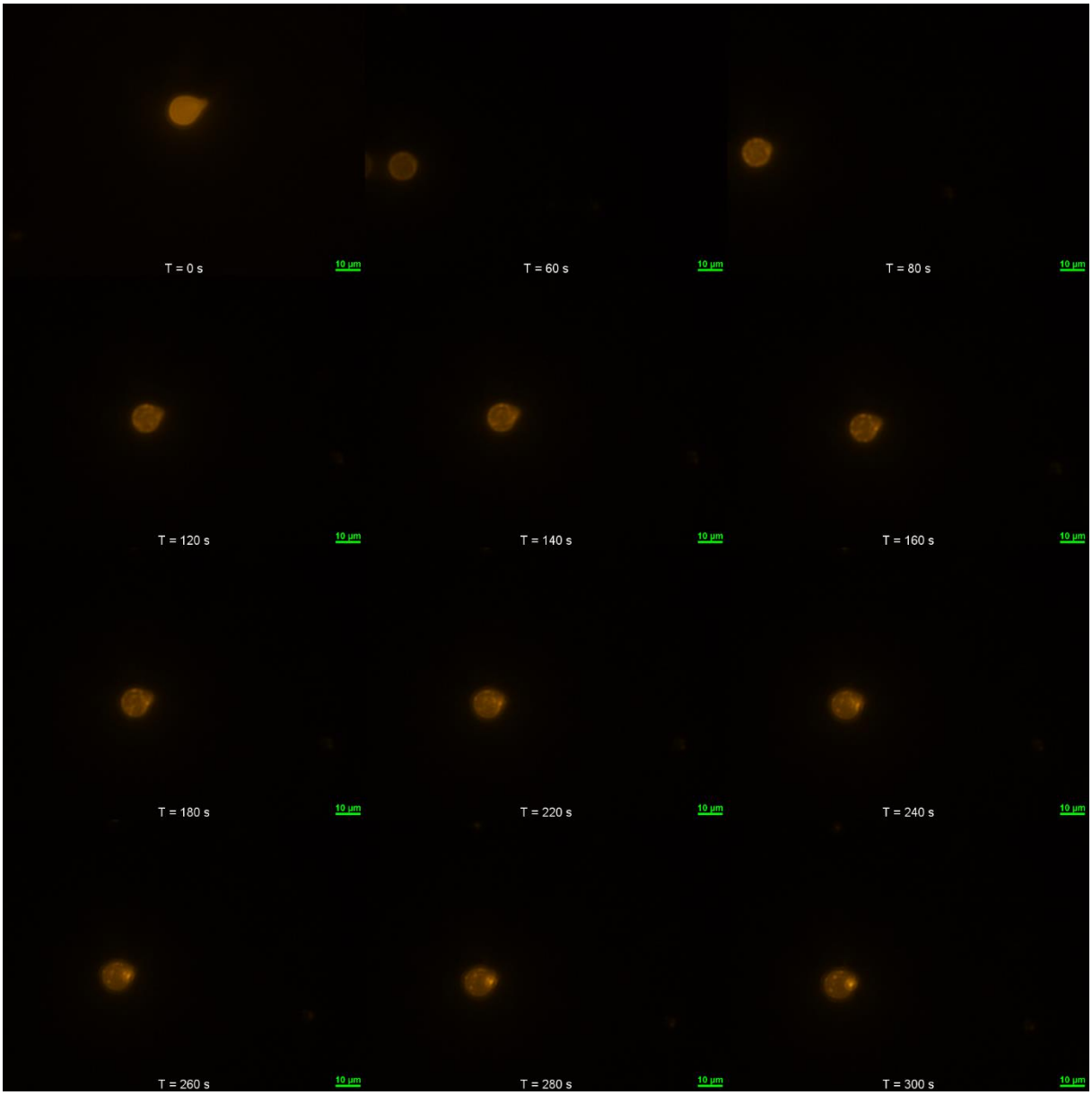

Figure B3. Time-lapse of a 30% Chol GUV. JR2KC-Cy5 were added around 20-30 seconds into the recording. The time-lapse was recorded as one image every 20 seconds for 5 minutes. GUV: 64.5:5:0.5:30 [POPC:MPB-PE:Liss-Rhod-PE:Chol], Filter: TRITC, Magnification: 60x, Exposure: 4 s, Analog gain: 1x, Shutter ND: 1.

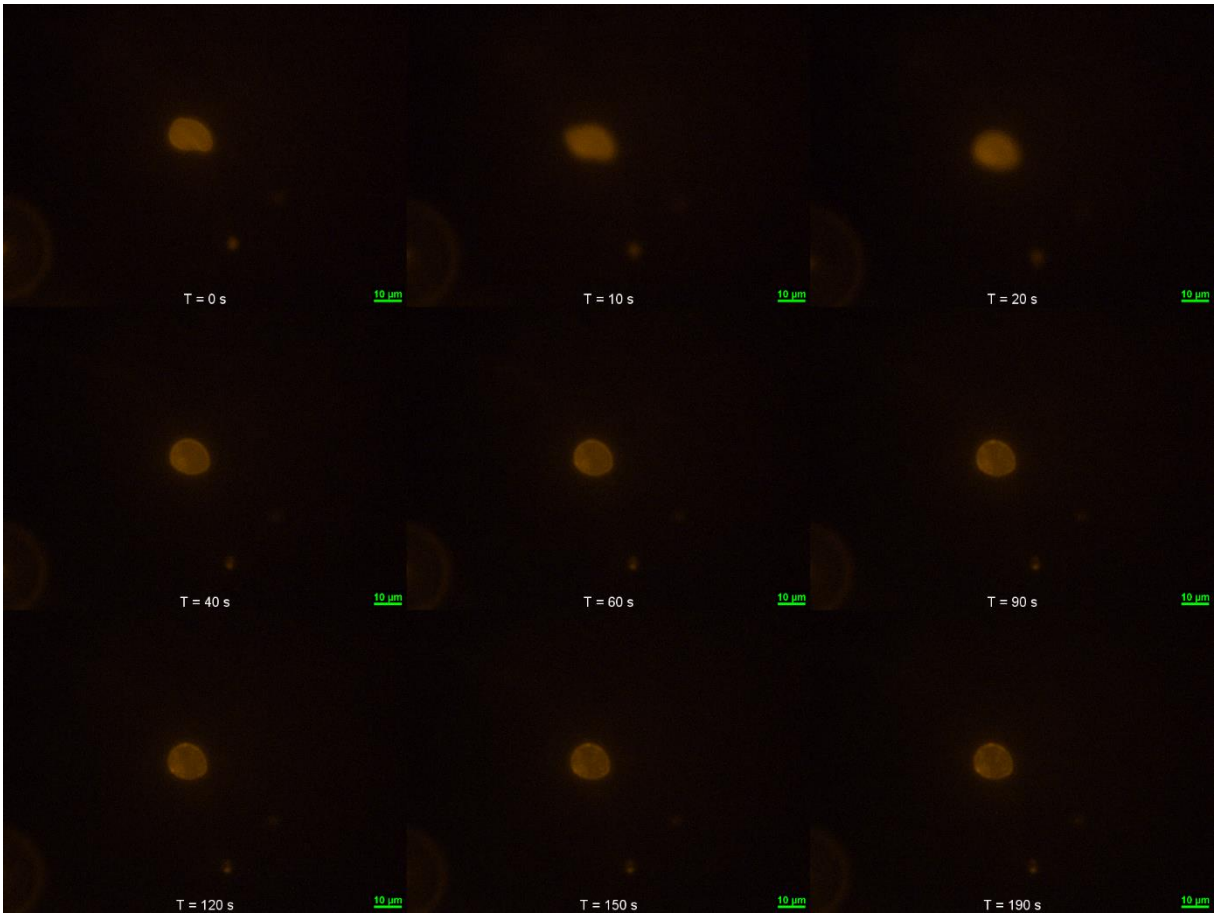

Figure B4. Time-lapse of a 30% Chol GUV. JR2KC-Cy5 were added around 10 seconds into the recording. The time-lapse was recorded as one image every 10 seconds for 3:10 minutes. GUV: 64.5:5:0.5:30 [POPC:MPB-PE:Liss-Rhod-PE:Chol], Filter: TRITC, Magnification: 60x, Exposure: 1 s, Analog gain: 4x, Shutter ND: 1.

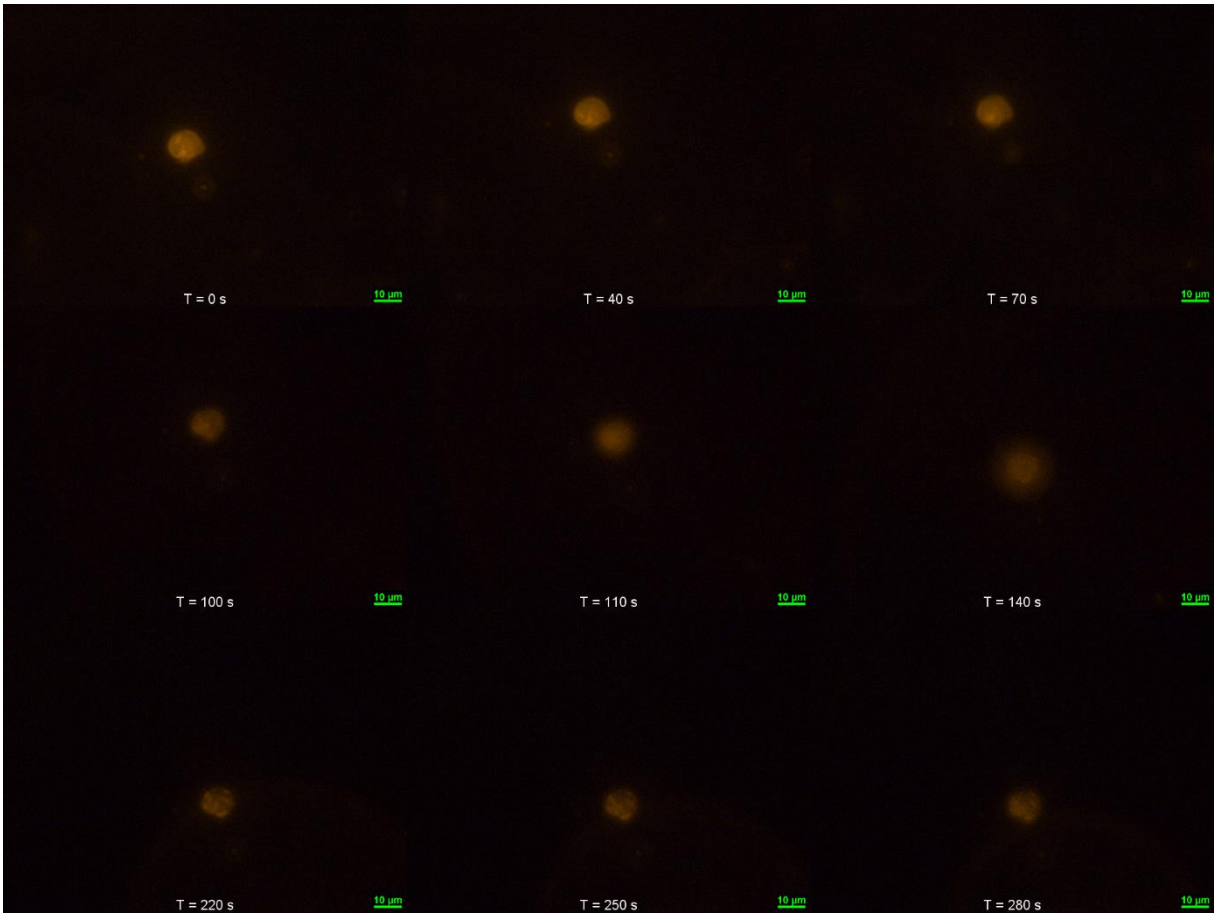

Figure B5. Time-lapse of a 30% Chol GUV. JR2KC-Cy5 were added around 80 seconds into the recording. The time-lapse was recorded as one image every 10 seconds for 5 minutes. GUV: 64.5:5:0.5:30 [POPC:MPB-PE:Liss-Rhod-PE:Chol], Filter: TRITC, Magnification: 60x, Exposure: 1 s, Analog gain: 4x, Shutter ND: 1.

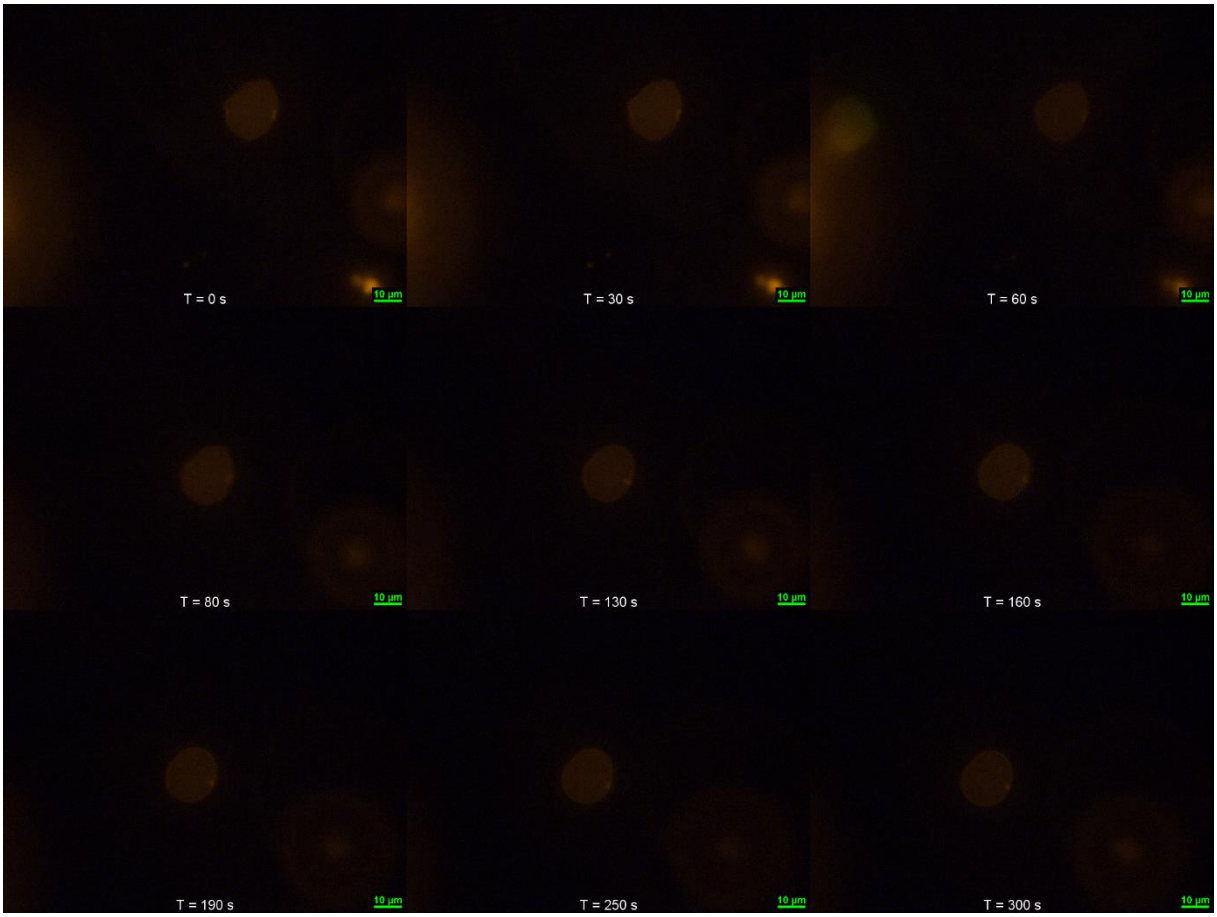

Figure B6. Time-lapse of a 30% Chol GUV. JR2K were added around 60 seconds into the recording. The time-lapse was recorded as one image every 10 seconds for 5 minutes. GUV: 64.5:5:0.5:30 [POPC:MPB-PE:Liss-Rhod-PE:Chol], Filter: TRITC, Magnification: 60x, Exposure: 1 s, Analog gain: 4x, Shutter ND: 1.

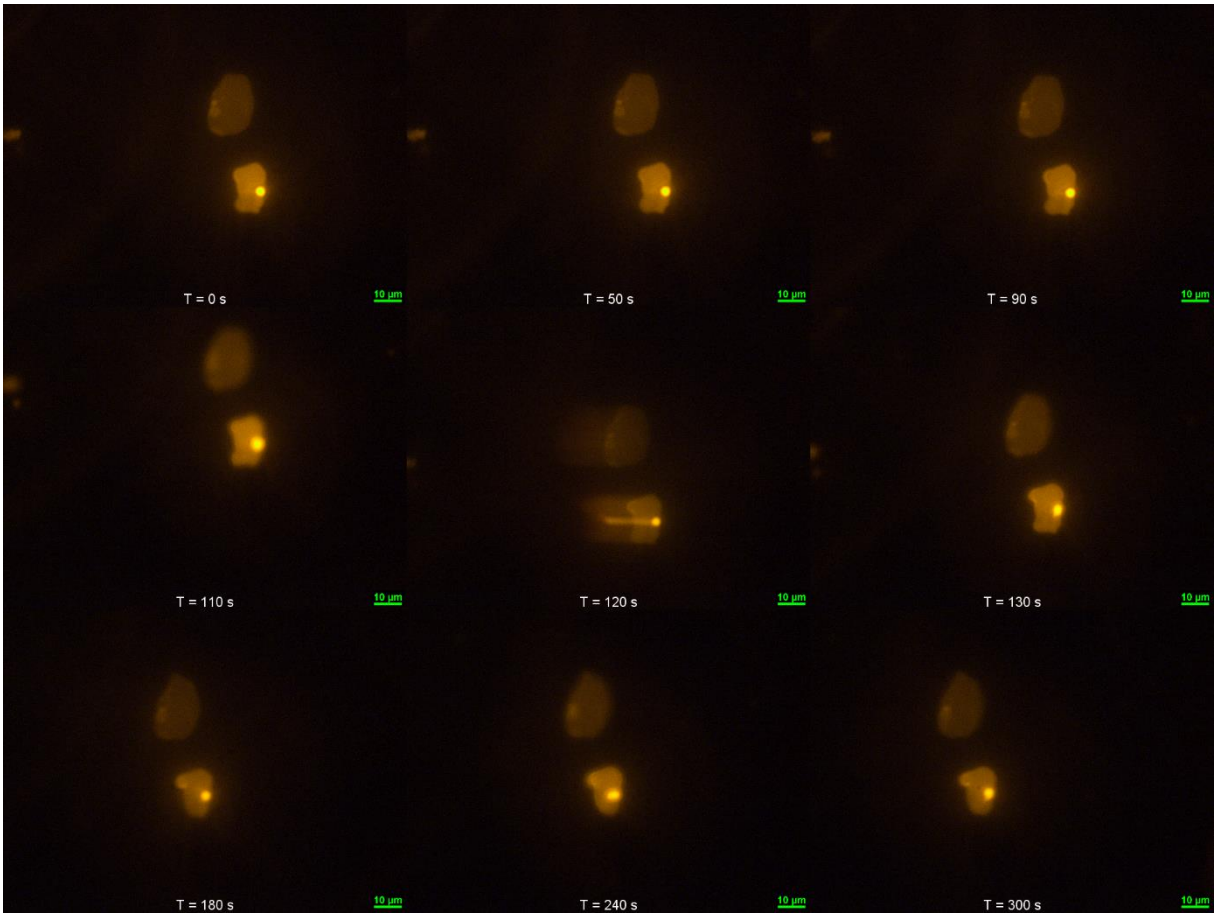

Figure B7. Time-lapse of a GUV without Chol. JR2K were added around 100 seconds into the recording. The time-lapse was recorded as one image every 10 seconds for 5 minutes. GUV: 94.5:5:0.5 [POPC:MPB-PE:Liss-Rhod-PE], Filter: TRITC, Magnification: 60x, Exposure: 1 s, Analog gain: 4x, Shutter ND: 1.

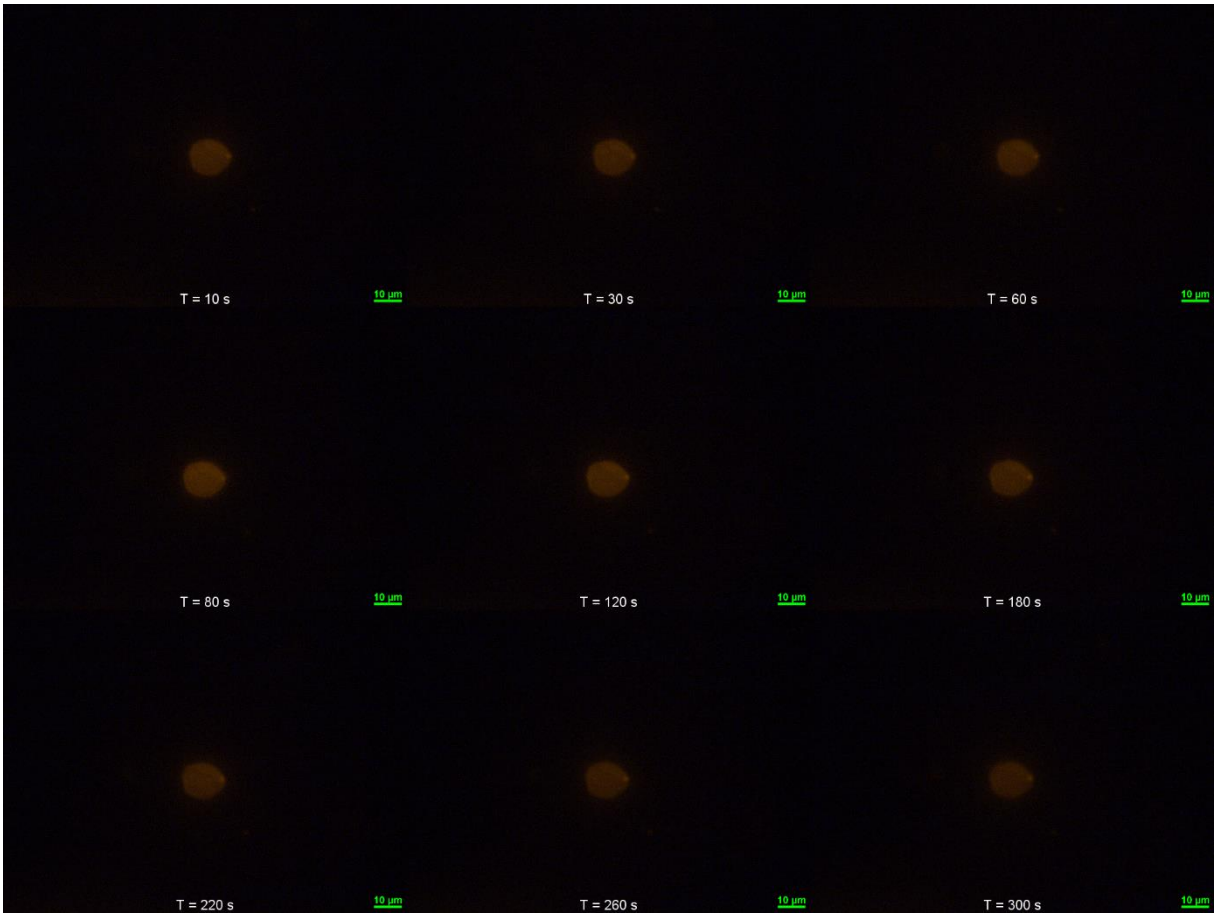

Figure B85. Time-lapse of a 30% Chol GUV. 1:1 [JR2KC-Cy5:pFTAA] mixture was added around 70 seconds into the recording. The time-lapse was recorded as one image every 10 seconds for 5 minutes. GUV: 64.5:5:0.5:30 [POPC:MPB-PE:Liss-Rhod-PE:Chol], Filter: TRITC, Magnification: 60x, Exposure: 1 s, Analog gain: 4x, Shutter ND: 1.

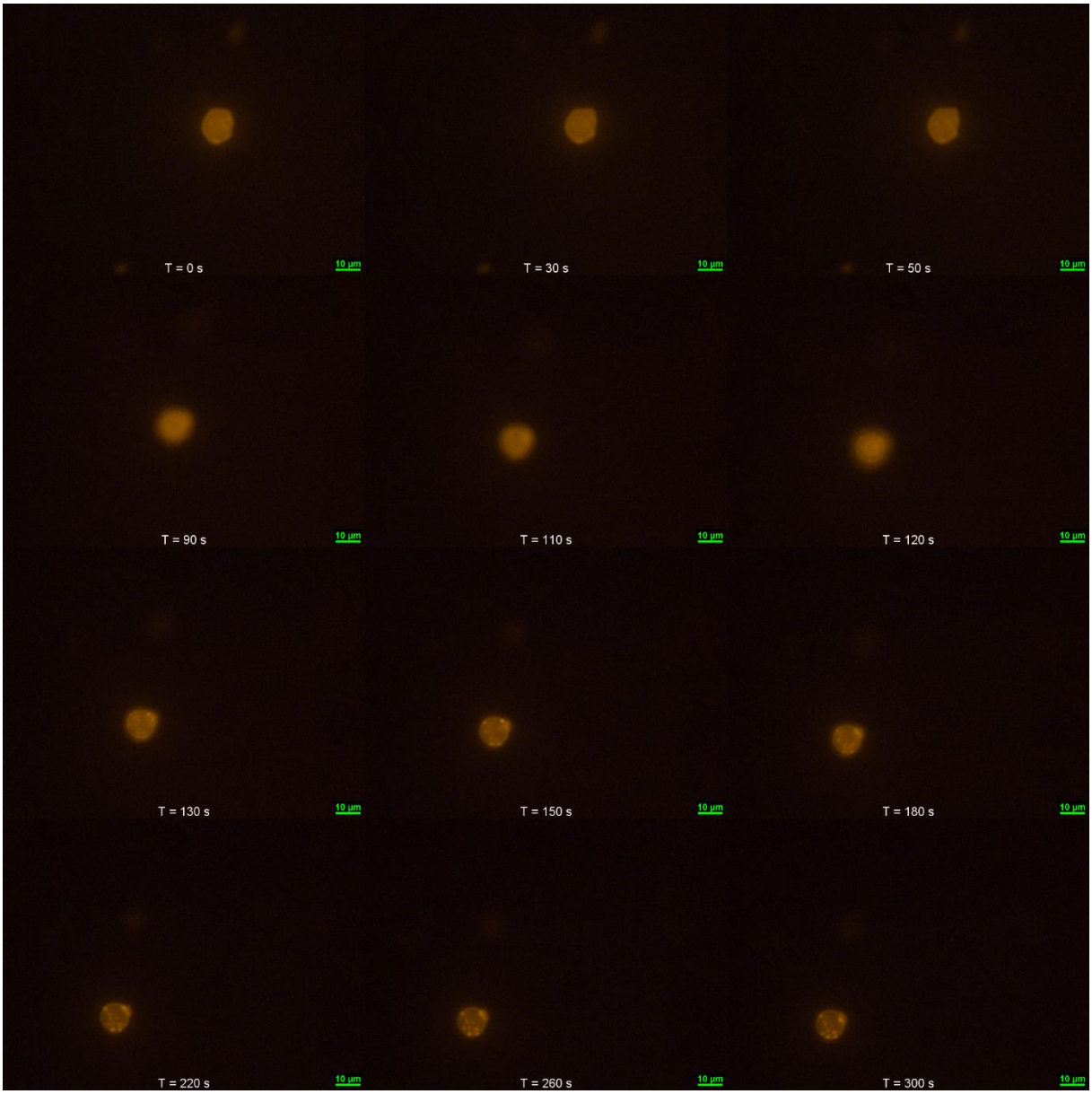

Figure B9. Time-lapse of a 30% Chol GUV. 1:1 [JR2KC-Cy5:pFTAA] mixture was added around 60 seconds into the recording. The time-lapse was recorded as one image every 10 seconds for 5 minutes. GUV: 64.5:5:0.5:30 [POPC:MPB-PE:Liss-Rhod-PE:Chol], Filter: TRITC, Magnification: 60x, Exposure: 2 s, Analog gain: 4x, Shutter ND: 1.

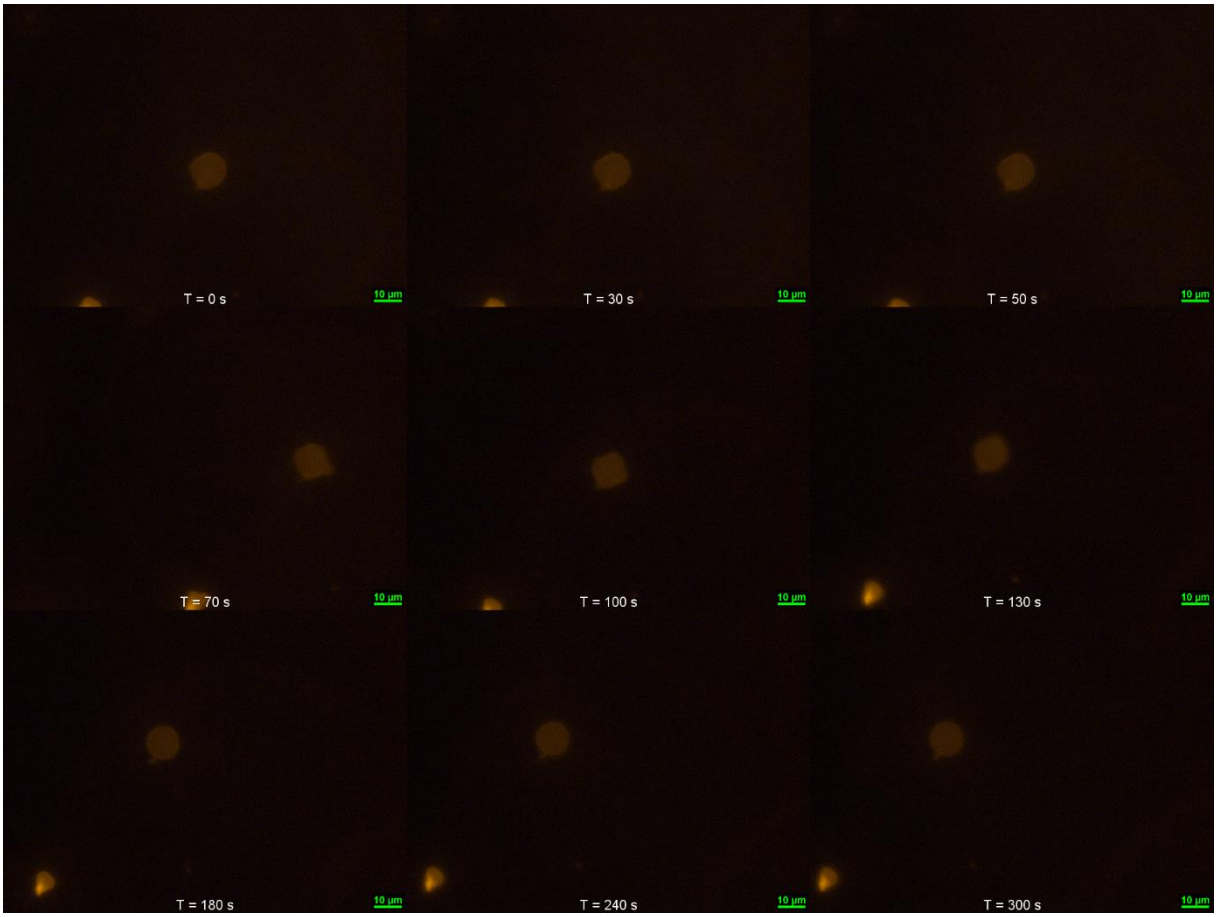

Figure B10. Time-lapse of a GUV without Chol. 1:1 [JR2KC-Cy5:pFTAA] mixture was added around 60 seconds into the recording. The time-lapse was recorded as one image every 10 seconds for 5 minutes. GUV: 94.5:5:0.5 [POPC:MPB-PE:Liss-Rhod-PE], Filter: TRITC, Magnification: 60x, Exposure: 1 s, Analog gain: 4x, Shutter ND: 1.

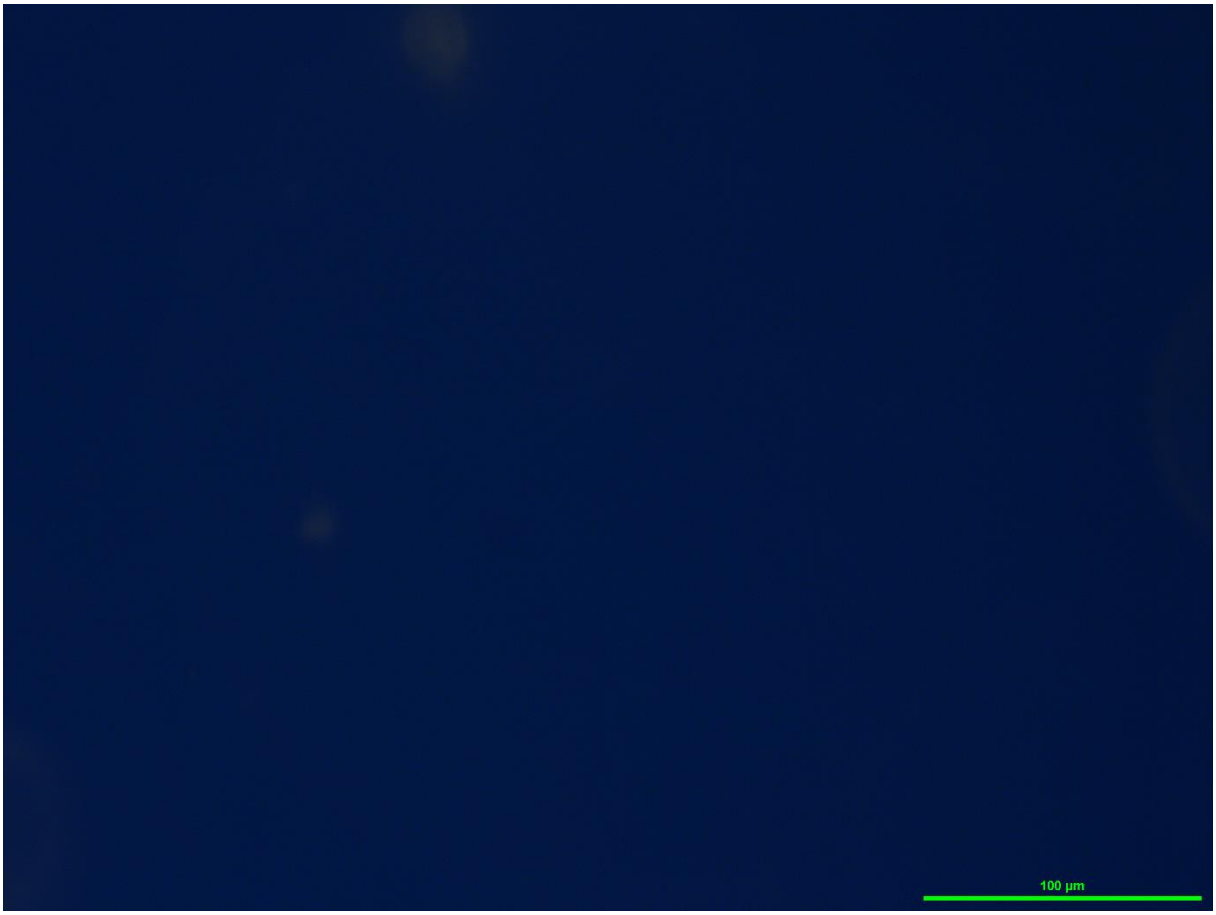

Figure B11. Image of well containing 30% Chol GUV. 1:1 [JR2KC-Cy5:pFTAA] mixture had not been added before the image was taken. GUV: 64.5:5:0.5:30 [POPC:MPB-PE:Liss-Rhod-PE:Chol], Filter: Aqua Longpass, Magnification: 20x, Exposure: 1 s, Analog gain: 1x, Shutter ND: 1.

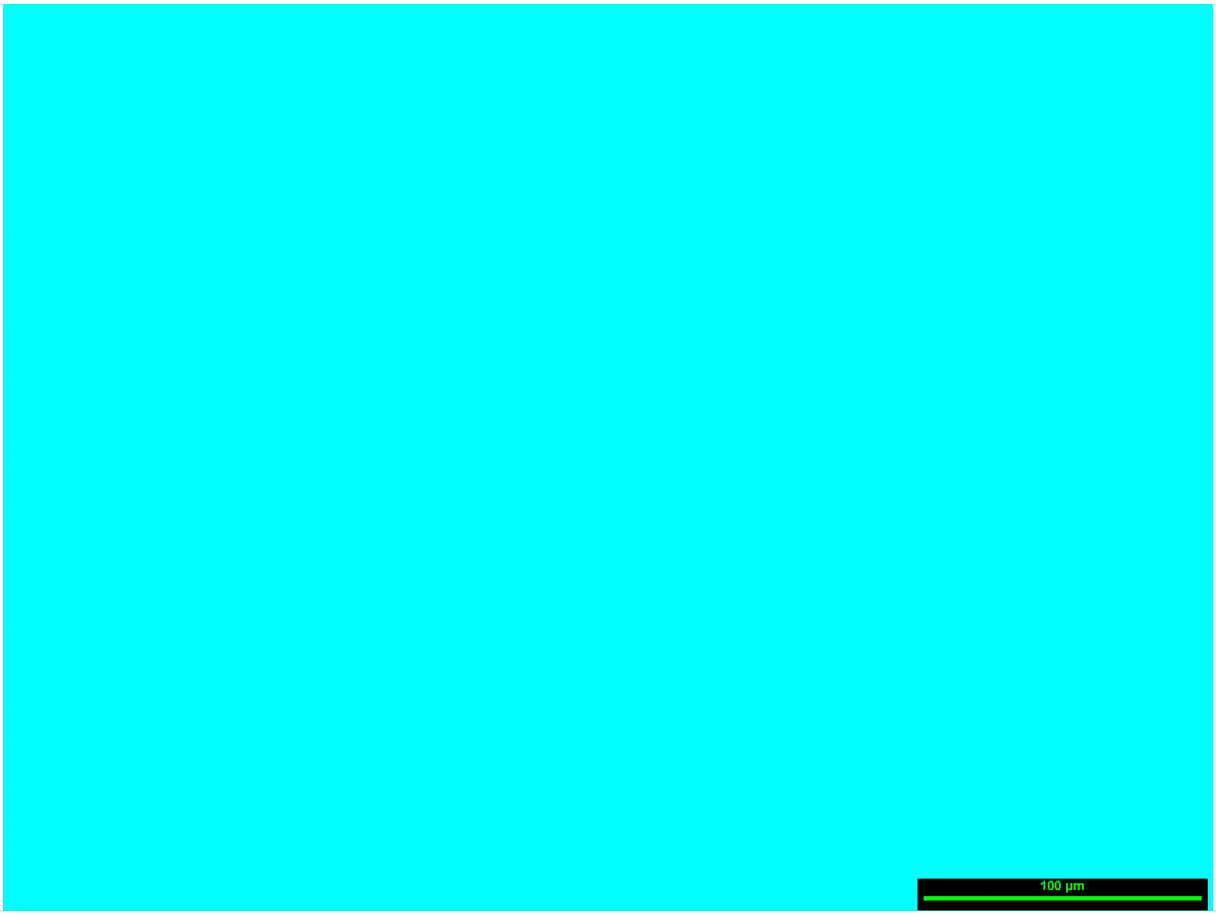

Figure B12. Image of well containing 30% Chol GUV after 1:1 [JR2KC-Cy5:pFTAA] mixture was added. GUV: 64.5:5:0.5:30 [POPC:MPB-PE:Liss-Rhod-PE:Chol], Filter: Aqua Longpass, Magnification: 20x, Exposure: 1 s, Analog gain: 1x, Shutter ND: 1.

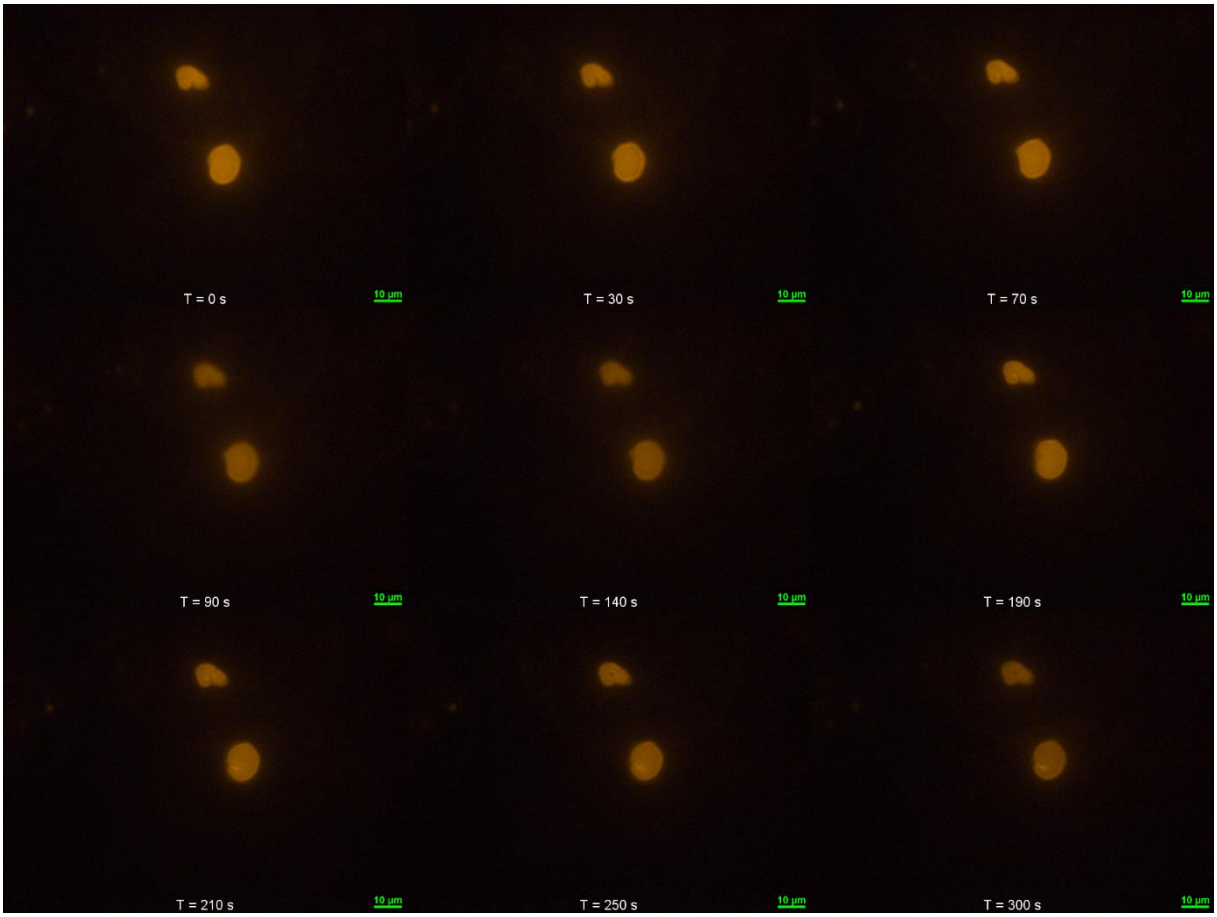

Figure B13. Time-lapse of a 30% Chol GUV. 1:20 [JR2KC-Cy5:pFTAA] mixture was added around 80 seconds into the recording. The time-lapse was recorded as one image every 10 seconds for 5 minutes. GUV: 64.5:5:0.5:30 [POPC:MPB-PE:Liss-Rhod-PE:Chol], Filter: TRITC, Magnification: 60x, Exposure: 2 s, Analog gain: 4x, Shutter ND: 1.

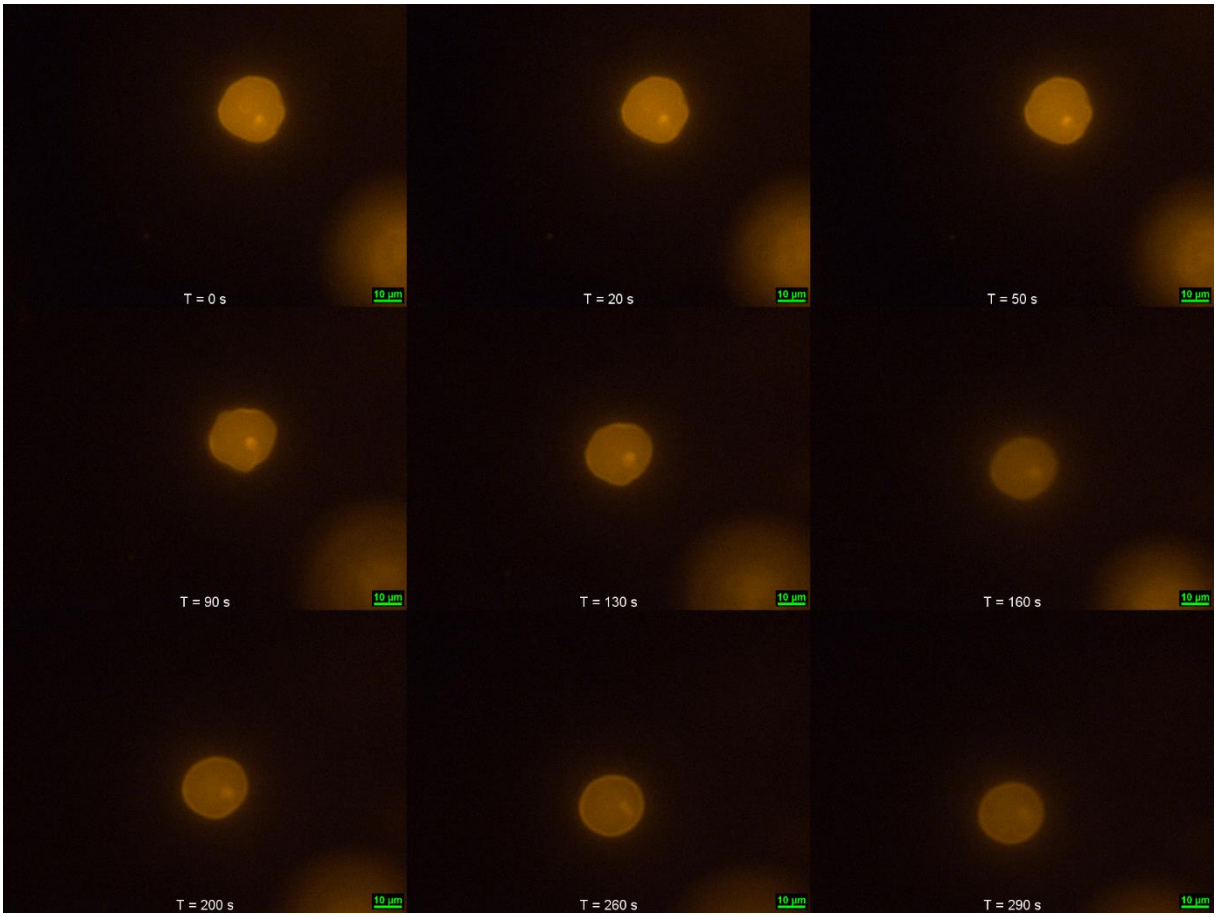

Figure B14. Time-lapse of a 30% Chol GUV. 1:20 [JR2KC-Cy5:pFTAA] mixture was added around 70 seconds into the recording. The time-lapse was recorded as one image every 10 seconds for 5 minutes. GUV: 64.5:5:0.5:30 [POPC:MPB-PE:Liss-Rhod-PE:Chol], Filter: TRITC, Magnification: 60x, Exposure: 2 s, Analog gain: 4x, Shutter ND: 1.

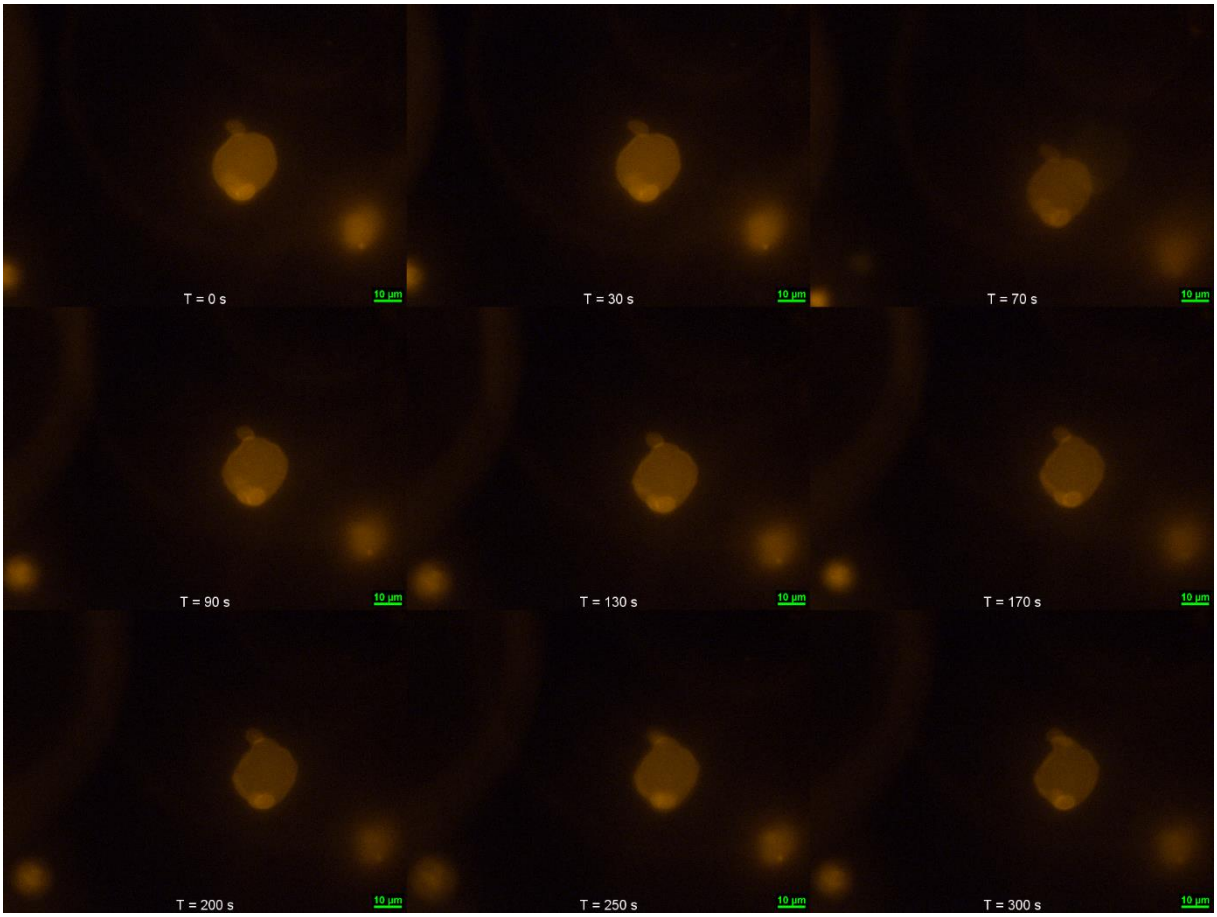

Figure B15. Time-lapse of a GUV without Chol. 1:20 [JR2KC-Cy5:pFTAA] mixture was added around 60 seconds into the recording. The time-lapse was recorded as one image every 10 seconds for 5 minutes. GUV: 94.5:5:0.5 [POPC:MPB-PE:Liss-Rhod-PE], Filter: TRITC, Magnification: 60x, Exposure: 1 s, Analog gain: 4x, Shutter ND: 1.

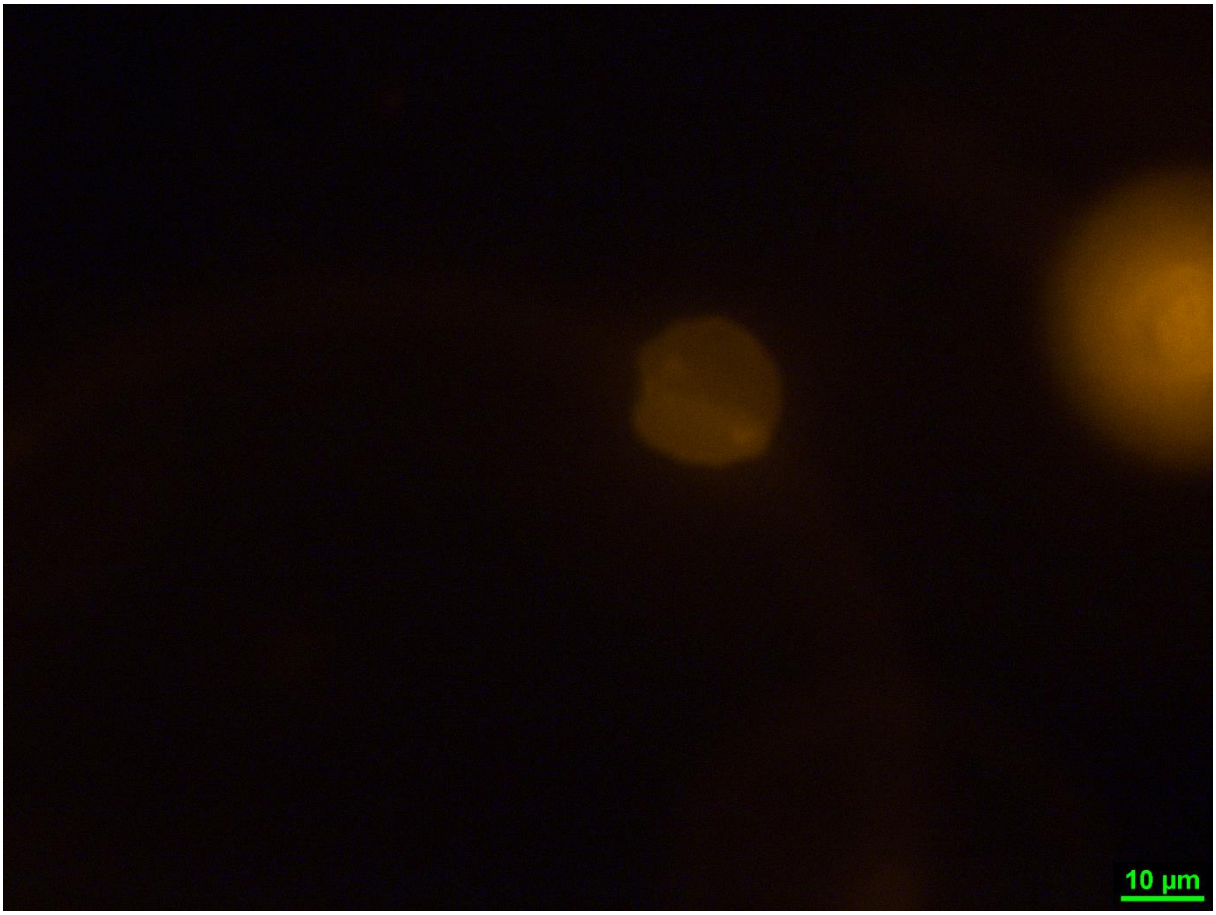

Figure B16. Image of a 30% Chol GUV 24 hours after 1:20 [JR2KC-Cy5:pFTAA] mixture was added. GUV: 64.5:5:0.5:30 [POPC:MPB-PE:Liss-Rhod-PE:Chol], Filter: TRITC, Magnification: 60x, Exposure: 1 s, Analog gain: 4x, Shutter ND: 1.

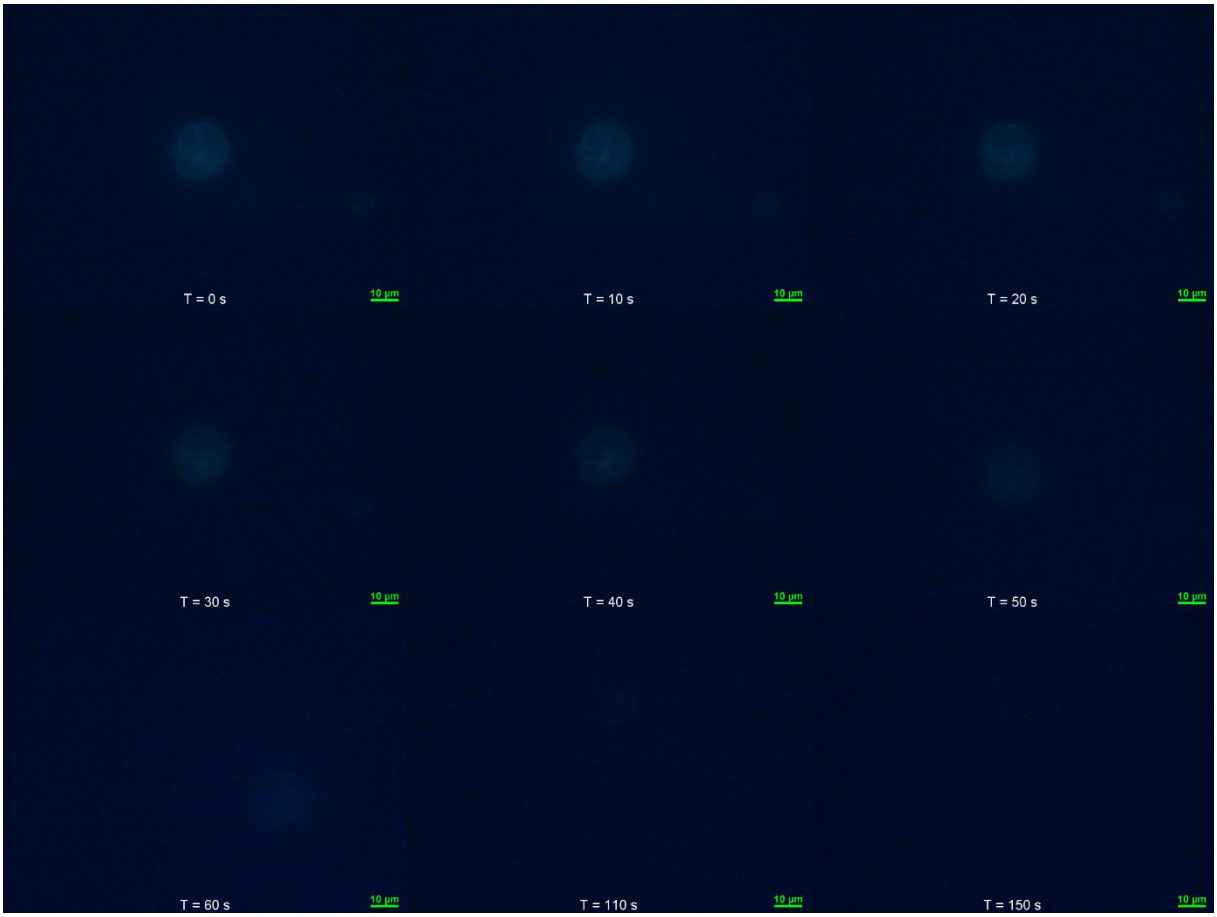

Figure B17. Time-lapse of a GUV containing Chol and pFTAA-Chol. The time-lapse was recorded as one image every 10 seconds for 3:10 minutes. GUV: 65:5:29.5:0.5 [POPC:MPB-PE:Chol:pFTAA-Chol], Filter: Aqua Longpass, Magnification: 60x, Exposure: 2 s, Analog gain: 4x, Shutter ND: 1.